

Supporting Information

Thermochemistry and Molecular Structure of a Remarkable Agostic Interaction in
a Heterobifunctional Ruthenium-Boron Complex

Brian L. Conley and Travis J. Williams*

Donald P. and Katherine B. Loker Hydrocarbon Research Institute and
Department of Chemistry, University of Southern California,
Los Angeles, California, 90089-1661
travisw@usc.edu

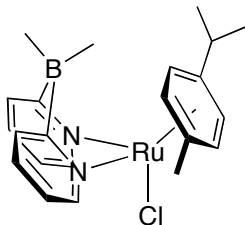
- I. General Procedures
- II. Experimental Details for New Compounds
- III. van't Hoff Analysis for Reversible Agostic Interaction
- IV. Rate Measurements and Thermochemical Analysis by ^1H NMR Inversion
Recovery/Magnetization Transfer
- V. Graphical ^1H and ^{13}C NMR Spectra for New Compounds
- VI. Oxidation of 1-(4-methoxyphenyl)ethanol
- VII. X-Ray Crystal Structure Solutions for **1**, **4**, and **7**

I. General Procedures

All air and water sensitive procedures were carried out either in a Vacuum Atmosphere glove box under nitrogen (2-10 ppm O₂ for all manipulations) or using standard Schlenk techniques under nitrogen. Labeled NMR solvents were purchased from Cambridge Isotopes Labs. Acetonitrile-*d*₃ (CD₃CN) and dichloromethane-*d*₂ (CD₂Cl₂) were dried over CaH₂; benzene-*d*₆ (C₆D₆) was dried over sodium benzophenone ketyl; acetone-*d*₆ was stored over activated 4 Å molecular sieves and all were vacuum transferred before use. NMR spectra were obtained on a Varian Mercury 400 MHz, Varian 400MR 400 MHz, or VNMRS 600 MHz spectrometer. All chemical shifts are reported in units of ppm and referenced to the residual ¹H solvent. NMR spectra were taken in 8" J-Young tubes (Wilmad). For protically sensitive molecules, the tubes were shaken vigorously for several minutes with chlorotrimethylsilane in hexanes then warmed gently with a heat gun under vacuum. Di-μ-chlorobis[(p-cymene)chlororuthenium(II)], min. 98% was purchased from Strem Chemicals. Dimethylbromoborane was purchased from Sigma Aldrich. 2-Bromopyridine was purchased from TCI America. *n*-Butyllithium (1.6 M in hexane) was purchased from Alpha Aesar. Sodium dimethylbis(2-pyridyl)borate, Na[(CH₃)₂B(py)₂] (**3**), was synthesized based on literature procedures.¹ Acetonitrile and acetonitrile-*d*₃ were refluxed over CaH₂ for 48 h, distilled, and then stored over 4 Å molecular sieves. Tetrahydrofuran was dried over sodium benzophenone ketyl. Silver trifluoromethane sulfonate was purchased from Sigma Aldrich or Strem Chemicals and used as received. Distilled water was purchased from Arrowhead and deoxygenated by purging with a stream of dry nitrogen. MALDI mass spectra were obtained on an Applied Biosystems Voyager spectrometer using the evaporated drop method on a coated 96 well plate. The matrix was anthracene. In a standard preparation, ~1 mg analyte and ~20 mg matrix were dissolved in a suitable solvent and spotted on the plate with a micro-pipetter. Standard C, H, N elemental analyses were performed by Desert Analytics Laboratory in Tucson, AZ, Galbraith Laboratories in Knoxville, TN, or University of Illinois, Urbana-Champaign. Fast atom bombardment (FAB) high-resolution mass spectra were collected at the University of California, Riverside Mass Spectrometry Facility and University of California, Los Angeles Molecular Instrumentation Center.

II. Experimental Details for New Compounds

Chlorocymene Ruthenium Complex 4:



In the glovebox, di- μ -chlorobis[(*p*-cymene)chlororuthenium(II)] (**2**, 100.0 mg, 0.163 mmol) was suspended (partially soluble) in 10 mL acetonitrile. $[\text{Na}(\text{CH}_3)_2\text{B}(\text{py})_2]$ (**3**, 71.9 mg, 0.326 mmol) in 10 mL acetonitrile was added dropwise and the solution was stirred for 0.5 h at room temperature under nitrogen. The orange solution was filtered over a celite/glass wool plug and then the solvent removed on a Schlenk line. The orange residue was treated with a minimal volume of benzene and quickly diluted with hexanes to generate an orange solid. The solution was decanted to yield **4** as a fine orange powder, 76.0 mg, 50% yield.

^1H NMR (400 MHz in benzene- d_6 at 25 °C): δ = 9.09 (dd, pyridyl 2H, J = 6.1 Hz), 7.92 (dd, pyridyl 2H, J = 7.5 Hz), 6.99 (dt, pyridyl 2H, J = 7.3 Hz), 6.46 (dt, pyridyl 2H, J = 6.6 Hz), 4.93 (d, cym 2H, J = 5.2 Hz), 4.61 (d, cym aromatic 2H, J = 4.8 Hz), 2.43 (septet, cym methane 1H, J = 7.1 Hz), 1.15 (s, cym methyl, 3H), 0.83 (d, cym isopropyl methyls 6H, J = 6.9 Hz), 0.75 (broad s, CH_3 -B 3H), 0.59 (broad s, CH_3 -B 3H).

^1H NMR (400 MHz in acetone- d_6 at 25 °C): δ = 9.01 (dd, pyridyl 2H, J = 6.1 Hz), 7.62 (dd, pyridyl 2H, J = 7.7 Hz), 7.46 (dt, pyridyl 2H, J = 8.0 Hz), 6.94 (dt, pyridyl 2H, J = 6.7 Hz), 5.57 (d, cym 2H, J = 6.0 Hz), 5.31 (d, cym aromatic 2H, J = 6.0 Hz), 2.79 (septet, cym CHMe_2 1H, J = 7.0 Hz), 1.73 (s, cym methyl, 3H), 1.21 (d, cym isopropyl methyls 6H, J = 6.9 Hz), 0.09 (broad s, overlapping CH_3 -B 6H).

^1H NMR (400 MHz in acetonitrile- d_3 at 25 °C): δ = 9.01 (dd, pyridyl 2H, J = 6.2 Hz), 7.68 (dd, pyridyl 2H, J = 7.8 Hz), 7.50 (dt, pyridyl 2H, J = 7.5 Hz), 6.98 (dt, pyridyl 2H, J = 6.4 Hz), 5.50 (d, cym 2H, J = 6.3 Hz), 5.25 (d, cym aromatic 2H, J = 6.0 Hz), 2.73 (septet, cym methyl 1H, J = 7.2 Hz), 1.67 (s, cym methyl, 3H), 1.15 (d, cym isopropyl methyls 6H, J = 6.6 Hz), 0.05 (broad s, CH_3 -B 6H).

$^{13}\text{C}\{^1\text{H}\}$ NMR (100 MHz in benzene- d_6 at 25 °C): δ = 155.45 (pyridyl), 134.17 (pyridyl), 130.15 (pyridyl), 119.70 (pyridyl), 104.75 (ipso cymene), 100.71 (ipso cymene), 86.54 (cym aromatic), 83.78 (cym aromatic), 30.25, 22.77, 17.09. Carbon atoms connected to boron were not observed directly due to broadening.

^{13}C shifts from HMQC (in acetonitrile- d_3 at 25 °C) δ = 158.26 (pyridyl), 135.80 (pyridyl), 130.72 (pyridyl), 121.67 (pyridyl), 87.10 (cym aromatic), 85.50 (cym aromatic), 31.04 (cym methine), 17.50 (cym methyl), 22.90 (cym i-Pr methyl), 16.20 (boron bound methyls).

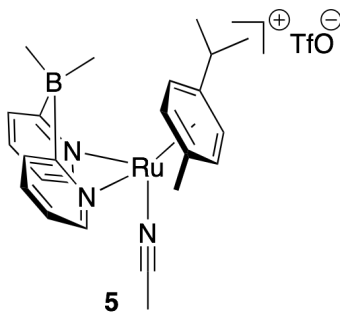
FAB HRMS for $[\text{M}-\text{Cl}]^+$: calc'd 433.1389 g/mol, found 433.1385 g/mol.

Elemental analysis: calc'd C: 56.48, H: 6.03, N: 5.99; found C: 55.93, H: 5.81, N: 6.36.

Infrared spectrum (cm^{-1}): ν = 2925 (s), 1592 (s), 1460 (s), 1384 (vs), 1287 (m), 996 (m), 865 (m), 759 (s), 750 (s).

Single crystal X-ray data for **4** are tabulated in section VII. CCDC 738030 contains the supplementary crystallographic data for this paper. These data can be obtained free of charge from The Cambridge Crystallographic Data Centre via www.ccdc.cam.ac.uk/data_request/cif

Cymene Ruthenium Triflate **5**:

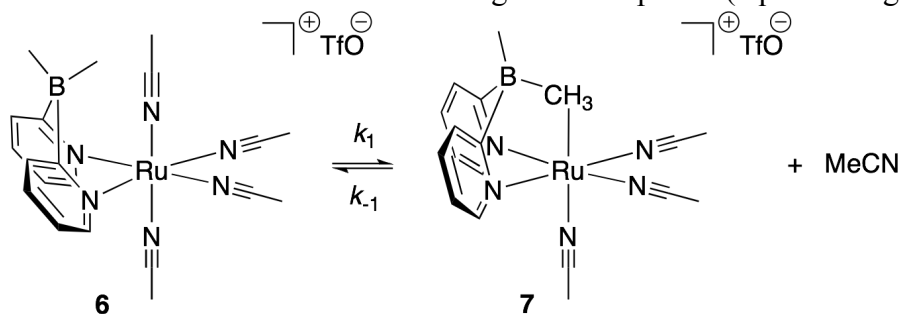


In the glovebox **4** (5.0 mg, 0.011 mmol) was shaken with silver triflate (3.0 mg, 0.012 mmol) in 0.5 mL CD₃CN in an 8" J-Young NMR tube that had been treated with Me₃SiCl and dried (see General Procedures). NMR data were taken within 5 minutes before significant acetonitrile/cymene substitution occurred.

¹H NMR (400 MHz in acetonitrile-*d*₃ at 25 °C): δ = 8.81 (dd, pyridyl 2H, *J* = 6.0 Hz), 7.81 (dd, pyridyl 2H, *J* = 8.0 Hz), 7.67 (dt, pyridyl 2H, *J* = 7.2 Hz), 6.53 (dt, pyridyl 2H, *J* = 6.5 Hz), 5.83 (d, cym 2H, *J* = 6.5 Hz), 5.57 (d, cym aromatic 2H, *J* = 6.5 Hz), 2.74 (septet, CHMe₂ 1H, *J* = 7.0 Hz), 1.72 (s, cym methyl, 3H), 1.17 (d, cym isopropyl methyls 6H, *J* = 6.9 Hz), 0.09 (broad s, CH₃-B 3H), 0.04 (broad s, CH₃-B 3H).

¹⁹F NMR (376 MHz in acetonitrile-*d*₃ at 25 °C): δ = -78. Only one ¹⁹F signal is observed through the duration of this transformation, which is consistent with an outer-sphere triflate.

Tetrakisacetonitrile Ruthenium Triflate **6** and Agostic Complex **7** (equilibrating mixture):



The J-Young tube containing **5** under nitrogen was heated in the NMR probe or a regulated silicone oil bath at 75 °C for ca. 5 minutes. This produces a solution of free *p*-cymene, **6** and **7**. Compound **6** is the predominant form at 75 °C (ca. 2:1 ratio). Data are determined from analysis of the equilibrated mixture based on peak integrations and several temperatures.

^1H NMR of **6** (400 MHz in acetonitrile- d_3 at 25 °C): δ = 8.66 (dd, pyridyl 2H, J = 7.0 Hz), 7.67 (broad d, pyridyl 2H, J = 7.6 Hz), 7.48 (dt, pyridyl 2H, J = 7.6 Hz), 6.92 (dt, pyridyl 2H, J = 6.7 Hz), 0.08 and 0.07 (overlapping broad s, CH_3 -B 6H).

^1H NMR of **7** (400 MHz in acetonitrile- d_3 at 25 °C): 8.55 (dd, pyridyl 2H, J = 5.7 Hz), 7.60 (dt, pyridyl 2H, J = 8.0 Hz), 7.44 (broad d, pyridyl 2H, J = 7.6 Hz), 7.06 (distorted t – overlapping free cymene signal, pyridyl 2H, J = 6.7 Hz), 0.18 (broad s, CH_3 -B 3H), -5.13 (broad s, Ru- CH_3 -B agostic 3H).

Selected ^{13}C shifts from HMQC in acetonitrile- d_3 : δ = -2.61 (CH_3 -B agostic, **7**), 8.1 (CH_3 -B unbound, **7**), 19.1 (CH_3 -B unbound, **6**), 196.0 and 197.1 (*ipso* pyridyls, **6**), 193.4 and 191.6 (*ipso* pyridyls, **7**), 119.8 (equatorial CH_3CN , **7**), 122.0 (equatorial CH_3CN , **6**). Aromatic region was frustrated by signals from **6**, **7**, **1**, and free cymene.

^{19}F NMR (376 MHz in acetonitrile- d_3 at 25 °C): δ = -78. Only one ^{19}F signal is observed through the duration of this transformation, which is consistent with an outer-sphere triflate.

Single crystal X-ray data for **7** are tabulated in section VII. CCDC 755444 contains the supplementary crystallographic data for this paper. These data can be obtained free of charge from The Cambridge Crystallographic Data Centre via www.ccdc.cam.ac.uk/data_request/cif

Determination of ligand environment of **6** and **7** in acetonitrile:

Because **6** and **7** are in situ-prepared compounds synthesized in acetonitrile- d_3 , acetonitrile ligands could not be determined in neat deuterated solvent. Further, the ^2H NMR signals were too broad to be useful. This disabled determination of the number of acetonitrile ligands in **6** and **7**, particularly whether the apical site in **6** was occupied by acetonitrile, which would have to be displaced in order for the agostic methyl to bridge to form. To probe the coordination sphere, we synthesized the compounds as above but substituted neat acetonitrile- d_3 for a 1:1 mixture of acetonitrile- d_3 and acetonitrile- h_3 , reasoning that all bound acetonitrile would be visible by ^1H NMR, be exactly 50% acetonitrile- d_3 acetonitrile- h_3 , and integrate appropriately to other proton peaks in their respective compounds by ^1H NMR. Spectra were taken using a Wet1D sequence to suppress acetonitrile- h_3 and examined in the region immediately downfield of free acetonitrile. Indeed, this analysis at 25 °C was diagnostic. Ligand peaks for **1** were identified at 2.56 and 2.44 ppm. We chose to execute this experiment on a sample of **6** + **7** that included a generous portion of **1** because **1** itself is a very useful integration standard because its *BMe* group has a similar T1 to *BMe* groups in **6** and **7**. In addition, four other major resonances were seen in the region: the peaks at 2.34 and 2.48 ppm integrate 1:1 with respect to each other and 1:2 with respect to the free dimethyl borate signal at 0.07 ppm for compound **6**. In a fully acetonitrile- h_3 molecule they would integrate 1:1 with the dimethyl signal. This establishes the presence of only 2 inequivalent ligands and indicates that the apical and axial bound acetonitriles are the same. Further, we believe that in a molecule inert to dimetallapyrimidine ring flipping, these signals would be resolved. Thus, these data suggest the ligand is ring flipping rapidly as is observed in an analogous platinum system.² In the same spectrum we see smaller peaks at 2.59 and 2.50 ppm that integrate 1:2 with respect to each other. The taller peak is assigned to the equatorial (6H) acetonitriles and integrates 1:1 with the unbound methyl in compound **7**. In a fully ring acetonitrile- h_3 molecule these would integrate 2:1 with this signal.

To further corroborate our assignments, we heated the NMR tube to 75 °C to observe the relative ratios of the peaks at 2.34, 2.48 (**6**), and 2.59, 2.50 (**7**) ppm. In accordance with our kinetic analyses (*vide infra*), the ligand peaks assigned to **7** grow in as those for **6** decrease (see *Figure S1*).

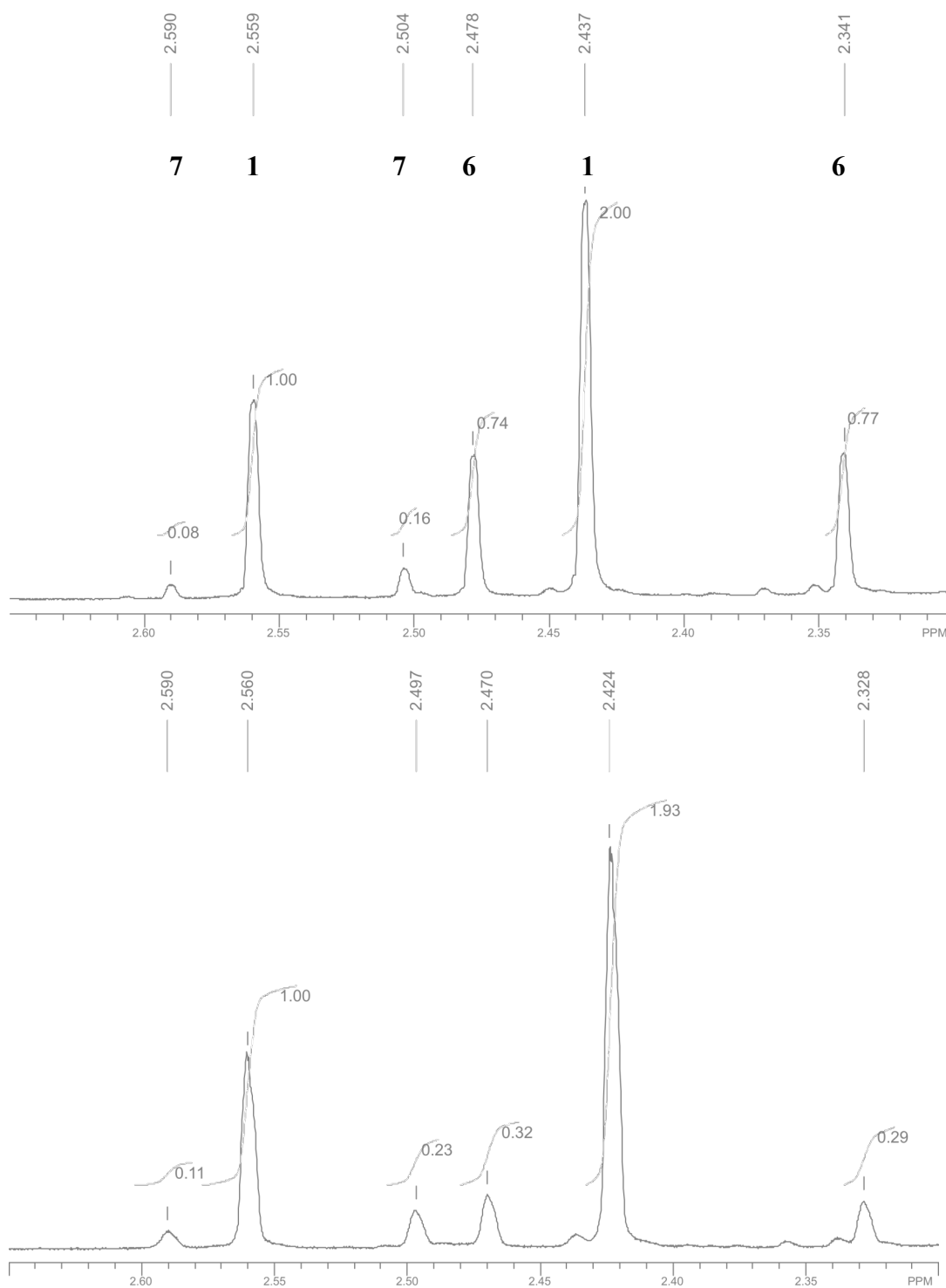
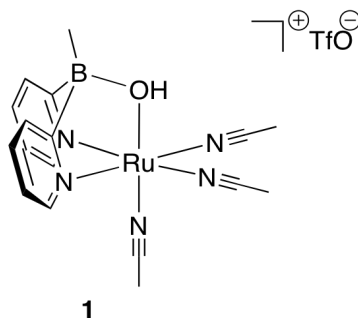


Figure S1. Bound Acetonitrile region of 400 MHz ¹H NMR Spectrum for an Equilibrating Mixture of **6** and **7** in 1:1 acetonitrile-*d*₃:acetonitrile-*h*₃. *Top:* at 25 °C. *Bottom:* at 75 °C. The relative increase of the peaks at $\delta = 2.56$ and 2.44 at higher temperature is due to hydrolysis (to **1**) by adventitious water in the NMR tube.

Trisacetonitrile μ -Hydroxide Ruthenium Triflate **1**:



In the glovebox, **4** (150.0 mg, 0.321 mmol) was dissolved in 10 mL acetonitrile in a 30 mL Straus flask that had been washed with distilled water and acetone and dried only briefly (ca. 10 minutes) on the Schlenk line, presumably leaving the glass well hydrated. To this solution was added AgOTf (86.5 mg, 0.337 mmol, 1.05 eq) in 5 mL acetonitrile. The solution was heated for 4 h at 75 °C, cooled to room temperature, then filtered over celite/glass wool in the glovebox. Solvent was removed and the residue dried overnight on the Schlenk line. The residue was re-dissolved in a minimum volume of dichloromethane and the resulting solution was diluted with hexanes, which resulted in the precipitation of a pale yellow solid. The solution was decanted and residual solvent was removed on the Schlenk line for several hours, yielding 115.1 mg (63% yield) of **1** as a light yellow material. This compound is air sensitive in solution and as a solid, yielding green paramagnetic (by ^1H NMR) material upon overnight exposure to the atmosphere.

^1H NMR (400 MHz in dichloromethane- d_2 at 25 °C): δ = 8.60 (dd, pyridyl 2H, J = 5.3 Hz), 7.56 (dt, pyridyl 2H, J = 7.8 Hz), 7.44 (dd, pyridyl 2H, J = 7.6 Hz), 7.05 (dt, pyridyl 2H, J = 6.6 Hz), 2.65 (s, axial CH_3CN , 3H), 2.49 (s, equatorial CH_3CN , 6H), 0.69 (s, -OH, 1H), 0.35 (s, $\text{CH}_3\text{-B}$ 3H).

^1H NMR (400 MHz in acetonitrile- d_3 at 25 °C): δ = 8.66 (dd, pyridyl 2H, J = 5.6 Hz), 7.59 (dt, pyridyl 2H, J = 7.8 Hz), 7.41 (dd, pyridyl 2H, J = 7.4 Hz), 7.07 (dt, pyridyl 2H, J = 6.5 Hz), 2.56 (s, axial CH_3CN , 3H), 2.44 (s, equatorial CH_3CN , 6H), 0.29 (s, $\text{CH}_3\text{-B}$ 3H, J_{HC} = 19.8 Hz).

$^{13}\text{C}\{^1\text{H}\}$ NMR (100 MHz in dichloromethane- d_2 at 25 °C): δ = 151.49 (pyridyl), 133.45 (pyridyl), 124.94 (pyridyl), 124.25 (axial CH_3CN), 123.78 (equatorial CH_3CN), 120.52 (pyridyl), 5.99 (axial CH_3CN), 5.54 (equatorial CH_3CN). Carbon atoms connected to boron were not observed directly due to broadening.

Selected ^{13}C shift from HMQC in acetonitrile- d_3 : δ = 3.32 ($\text{CH}_3\text{-B}$).

FAB HRMS for $[\text{M-OTf}]^+$: calc'd 424.0883 g/mol, found 424.0863 g/mol. Elemental analysis: calc'd C: 37.77, H: 3.70, N: 12.24; found C: 37.53, H: 3.53, N: 12.01.

Infrared spectrum (cm^{-1}): ν = 3439 (m), 2272 (m), 1457 (m), 1428 (m), 1265 (vs, triflate), 1225 (s), 1156 (vs), 1031 (vs, triflate), 772 (m), 637 (vs, triflate).

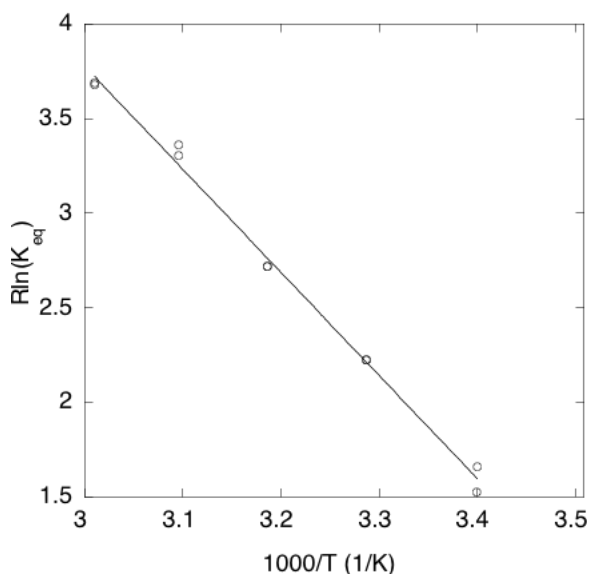
Single crystal X-ray data for **1** are tabulated in section VII. CCDC 738031 contains the supplementary crystallographic data for this paper. These data can be obtained free of charge from The Cambridge Crystallographic Data Centre via www.ccdc.cam.ac.uk/data_request/cif

III. van't Hoff Data for Reversible Agostic Interaction

Measurement of K_{eq} was conducted by integrating methyl peaks downfield of 0 ppm in an equilibrating mixture of **6** and **7** (generated in situ as described above). Probe temperature was cycled from 20 °C to 60 °C by 10 °C increments and then back down in the same manner to collect two data points for each temperature. The temperature was calibrated using shift difference measurements in methanol and ethylene glycol standards. Three measurements were taken at each value and the temperature reported as the average. Error in ΔH and ΔS were calculated by linear regression analysis using Kaleidagraph software.

Table S1. K_{eq} Measurement and van't Hoff Analysis for B-CH₃ Agostic Interaction Formation (Compounds **6** and **7**). $\Delta H = 5.5(2)$ kcal/mol and $\Delta S = 20.1(5)$ eu.

Run	Temp (°C)	K_{eq} (M)
1	21.0(2)	2.15
2	21.0(2)	2.46
1	31.1(2)	3.06
2	31.1(2)	3.06
1	40.7(2)	3.93
2	40.7(2)	3.93
1	49.9(2)	5.27
2	49.9(2)	5.57
1	59.1(2)	6.37
2	59.1(2)	6.43



Please note that K_{eq} has units of M; $K_{eq} = [7][MeCN][6]^{-1}$. For comparative purposes, **6**: **7** = 1: 1 at 90 °C even though K_{eq} (90 °C) = 19(1) M because $[MeCN] = 19$ M.

IV. Rate Measurements and Thermochemical Analysis by ^1H NMR Inversion Recovery/Magnetization Transfer

In order to obtain rate constants and activation parameters for the chemical exchange of methyl groups in compounds **6** and **7**, an *in situ* equilibrium was set up in a sealed J. Young NMR tube as described above. A soft-pulse inversion recovery sequence was fashioned by calibrating VNMRJ's built-in Presat sequence to match a known protocol used for intramolecular isomerization applications.³ The methyl peak at -5.15 ppm (bridging methyl in **7**, 3H) was selectively inverted with a calibrated soft pulse, which was determined by arraying the soft pulse width. Next, the interpulse delay time arrayed (20-45 values ranging from ca. 0 to 10 sec.) and the experiment was initiated. The complementary +0.07 ppm methyl peak (unbound dimethyl borate in **6**, 6H) was integrated in each spectrum against an internal standard using VNMRJ processing software. Data were plotted as a function of the interpulse delay (**Figure S3**).

The raw data were fit to a two-site model⁴ using the freeware processing program CIFIT.⁵ Resulting values for equilibrium magnetization and exchange rate constants were recorded. A van't Hoff plot (**Figure S4**) derived from equilibrium magnetization values is in statistical agreement with the one above ($\Delta H = 5.7(2)$ kcal/mol; $\Delta S = 21.9(6)$ eu). Observed exchange rate constants were corrected to account for the apparent double integration of the 6H signal. Eyring plots to determine ΔH^\ddagger and ΔS^\ddagger were constructed from the measured rate constants (**Table S2** and **Table S3**).

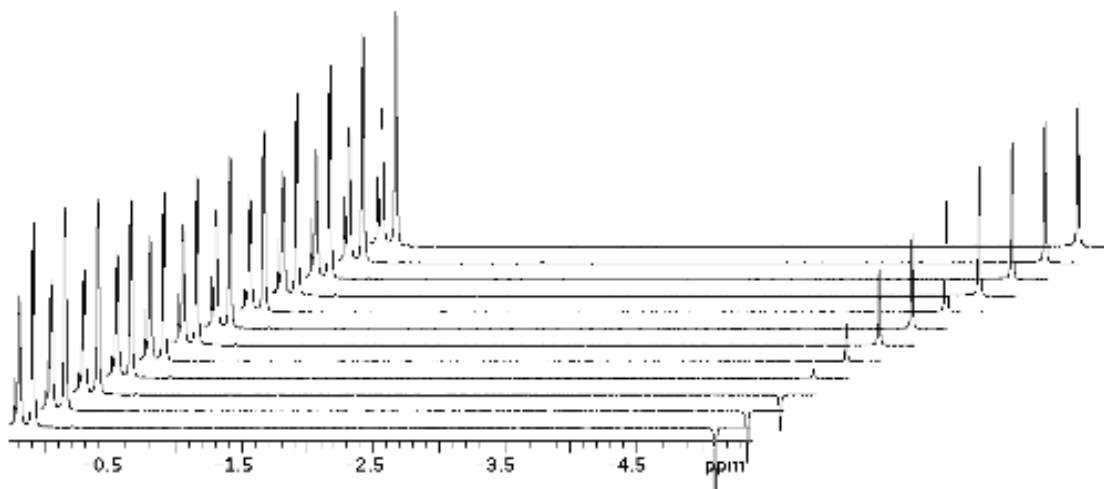


Figure S2. Demonstration Inversion-Recovery Data Collected on a Varian VNMRs 600 at 84.8 °C with interpulse delays arrayed between 50 ms to 7 s in this sampling.

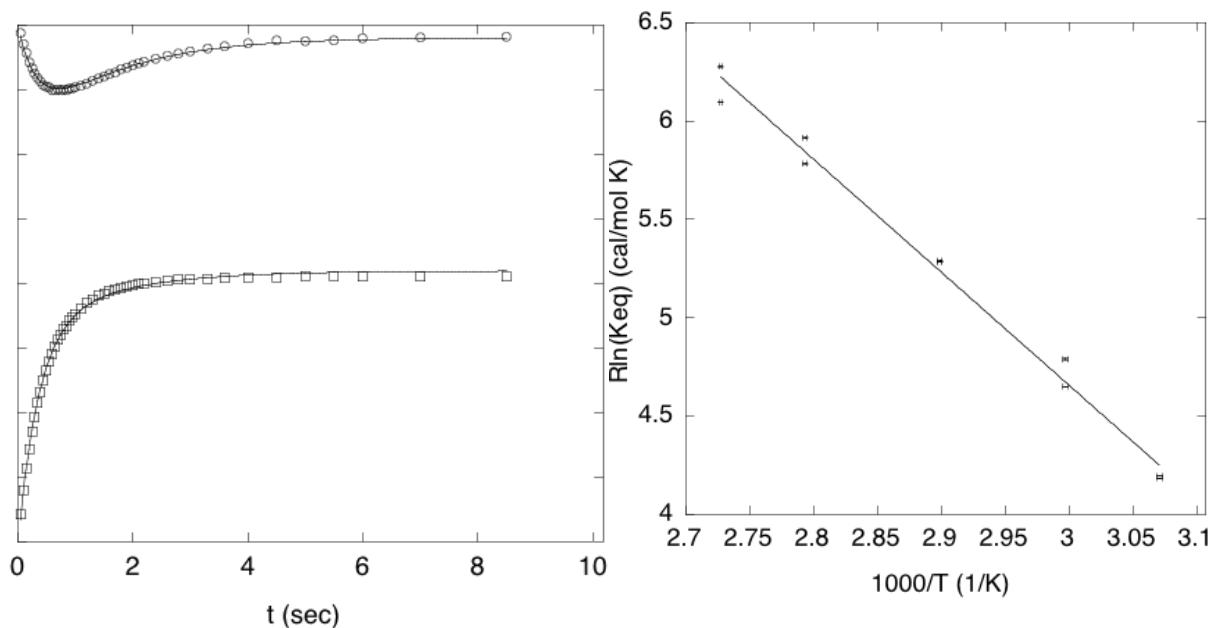


Figure S3. Representative Example of Processed Selective Inversion Recovery Magnetization Transfer Data. Integration of ^1H NMR signals for unbound dimethyl boron (top, 0.07 ppm) and bridging methyl (bottom, -5.15 ppm) vs. delay time (d2, s) before detection. Sample temperature was 72 °C. Bridging methyl signal was irradiated with a calibrated pulse.

Figure S4. van't Hoff Plot Constructed from Fitted Values of Equilibrium Magnetization. $\Delta H = 5.7(2)$ kcal/mol; $\Delta S = 21.9(6)$ eu.

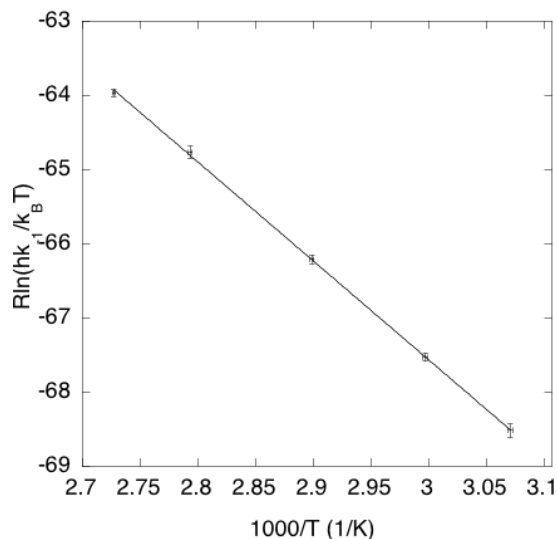
Table S2. Rate Constants ($k_{-1 \text{ obs}}$, k_{-1}) and Eyring Plot for the Conversion of **7** to **6**.

T (°C)	$k_{-1 \text{ obs}}$ (s ⁻¹)	$k_{-1} \times 10^{-3}$ (M ⁻¹ s ⁻¹)
52.5(2)	0.14(1)	7.2(3)
60.5(2)	0.23(1)	12.1(3)
71.8(2)	0.46(1)	24.2(7)
84.8(2)	0.98(4)	52(2)
93.5(2)	1.51(4)	80(2)

Error bars represent quality of fit only.

$$\Delta H^\ddagger = 13.3(6) \text{ kcal/mol}$$

$$\Delta S^\ddagger = -27.5(43) \text{ eu.}^6$$



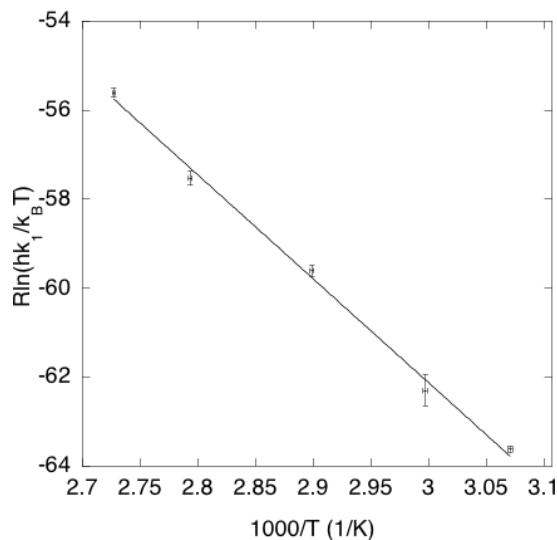
A second set of data was collected exactly as described above, but with inversion of the 6H signal at + 0.07 ppm (unbound dimethyl borate in **6**). In these data, NOE transfer of magnetization and/or unselective inversion are problematic because of the proximity of the signal for **7**'s free boron methyl at + 0.18 ppm. In such cases, $\Delta\delta$ must be much larger than τ_A^{-1} and τ_B^{-1} , where τ is the observed lifetime in the site.⁷ In our case we have $\Delta\delta = 44$ Hz; $\tau_A^{-1} = 7 \text{ sec}^{-1}$; and $\tau_B^{-1} = 12 \text{ sec}^{-1}$. Thus, this experiment must be taken as an estimate. For completion's sake, the results follow.

Table S3. Estimated First Order Rate Constants (k_1) and Eyring Plot for the Conversion of **6** to **7**.

T (°C)	k_1 (s ⁻¹)
52.5(2)	0.084(3)
60.5(2)	0.17(3)
71.8(2)	0.67(4)
84.8(2)	1.99(16)
93.5(2)	5.37(29)

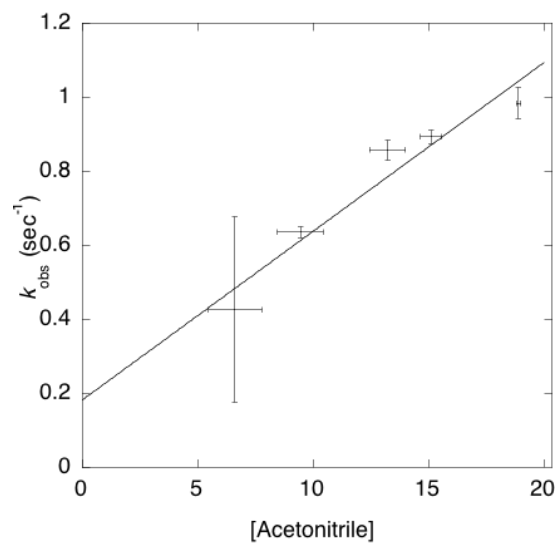
Error bars represent quality of fit only.

$\Delta H^\ddagger \sim 23 \text{ kcal/mol}$; $\Delta S^\ddagger \sim 8 \text{ eu}$. ΔH^\ddagger appears to be an over estimate.

**Table S4.** Dependence of k_{obs} (s⁻¹) for Conversion of **7** to **6** on Acetonitrile Concentration (M).

[acetonitrile] (M)	$k_{-1 \text{ obs}}$ (s^{-1})
18.9(1)	0.98(4)
15.1(5)	0.89(2)
13.2(8)	0.86(3)
9.5(10)	0.64(1)
6.6(12)	0.43(25)

Error bars represent quality of fit only.
Acetonitrile concentration was reduced
by adding aliquots of benzene- d_6 .



V. Graphical ^1H and ^{13}C NMR Spectra for New Compounds

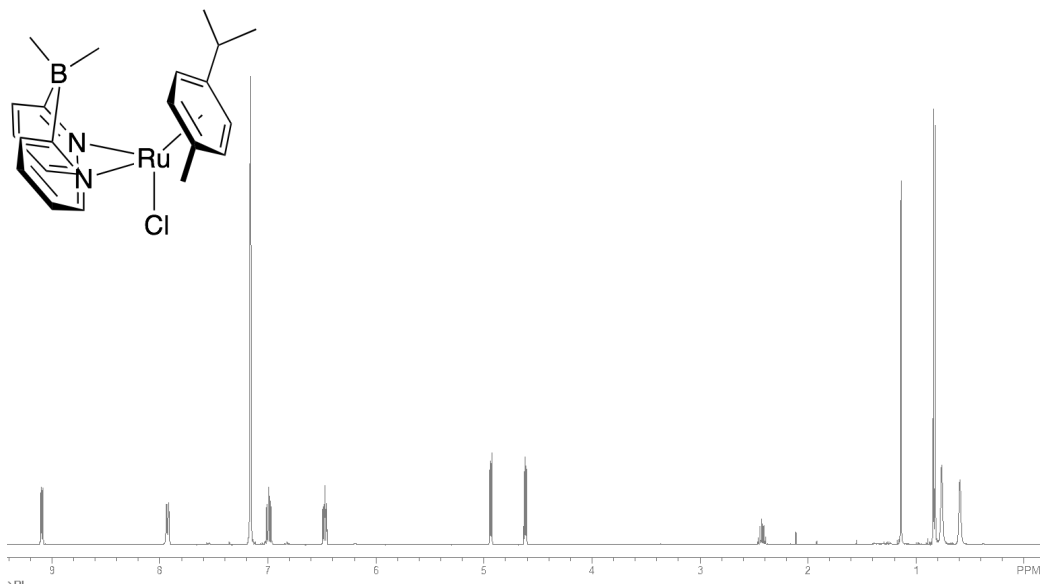


Figure S5. 400 MHz ^1H NMR of Compound 4 in Benzene- d_6 .

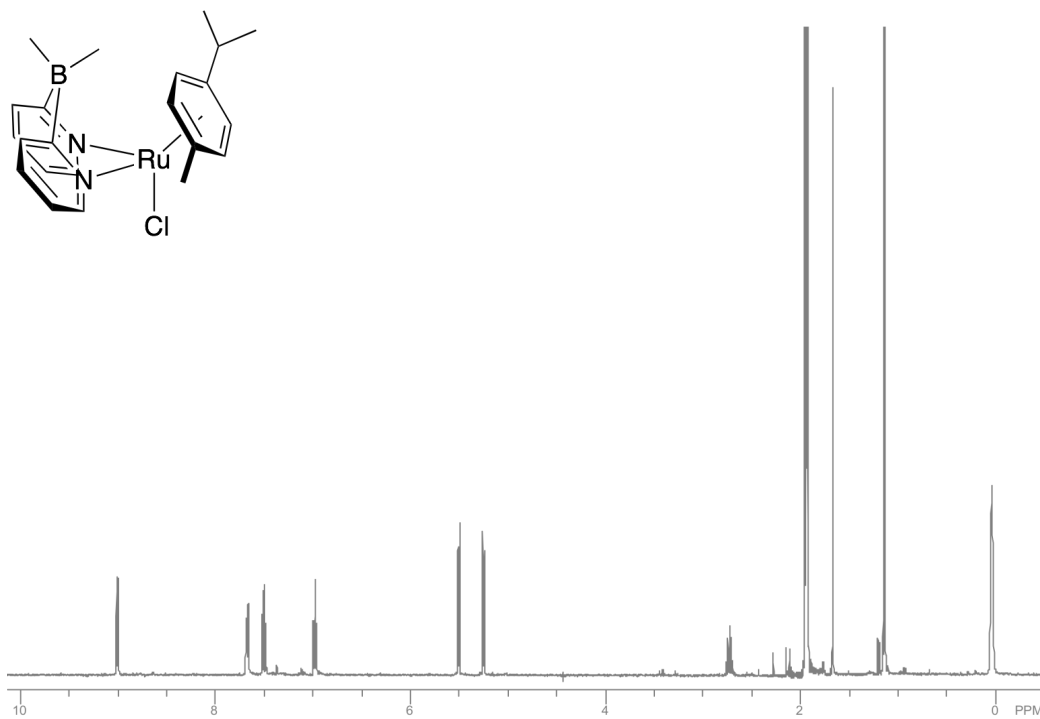


Figure S6. 400 MHz ^1H NMR Compound 4 in Acetonitrile- d_3 .

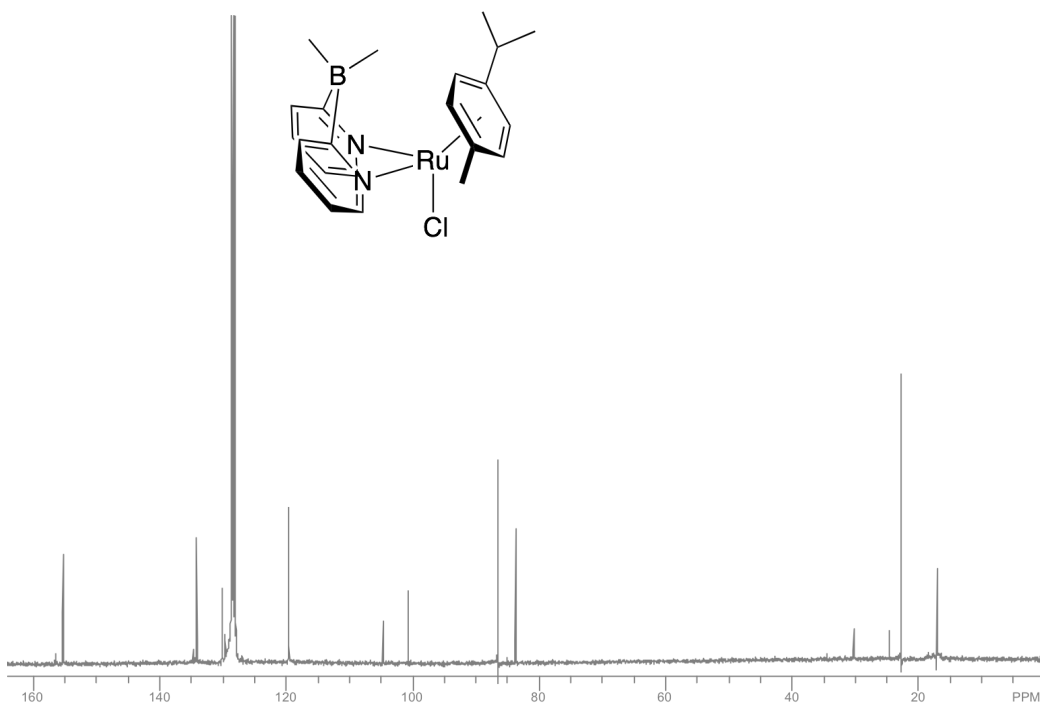


Figure S7. 100 MHz $^{13}\text{C}\{^1\text{H}\}$ NMR of Compound **4** in Benzene- d_6 .

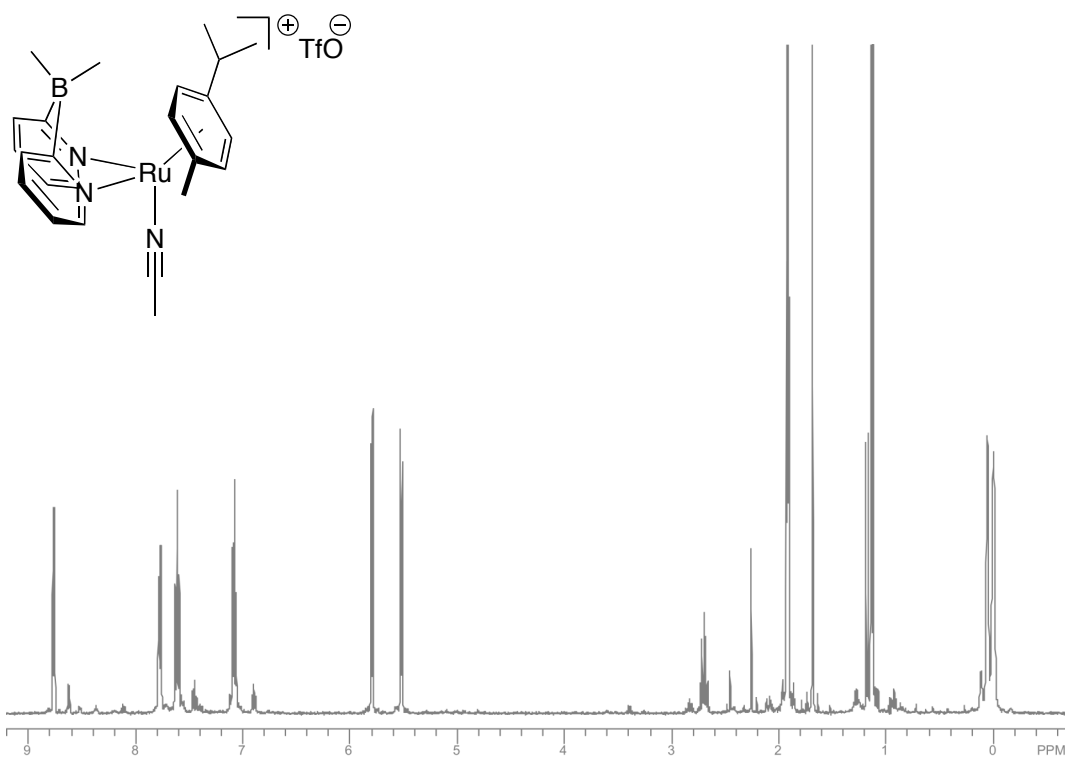


Figure S8. 400 MHz ^1H NMR Compound **5** in situ in Acetonitrile- d_3 .

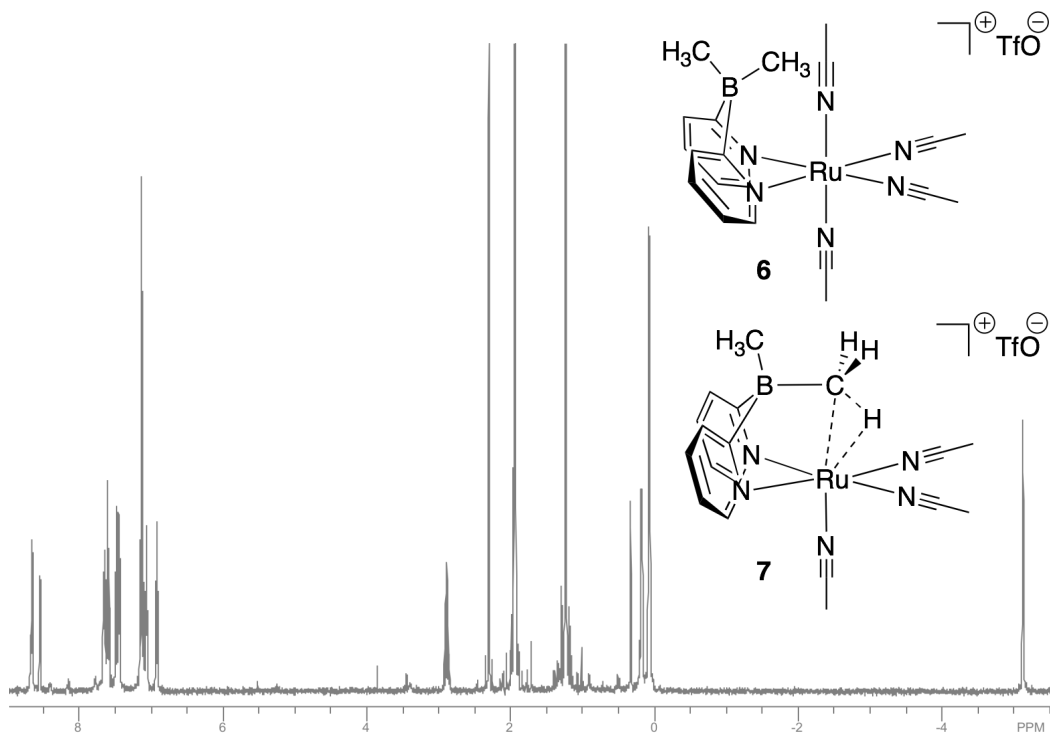


Figure S9. 400 MHz ^1H NMR of **6** and **7** Equilibrating in Acetonitrile- d_3 at $75\text{ }^\circ\text{C}$. Upfield methyl peak at 0.36 ppm is **1** resulting from residual H_2O . Methane is 0.23 ppm .

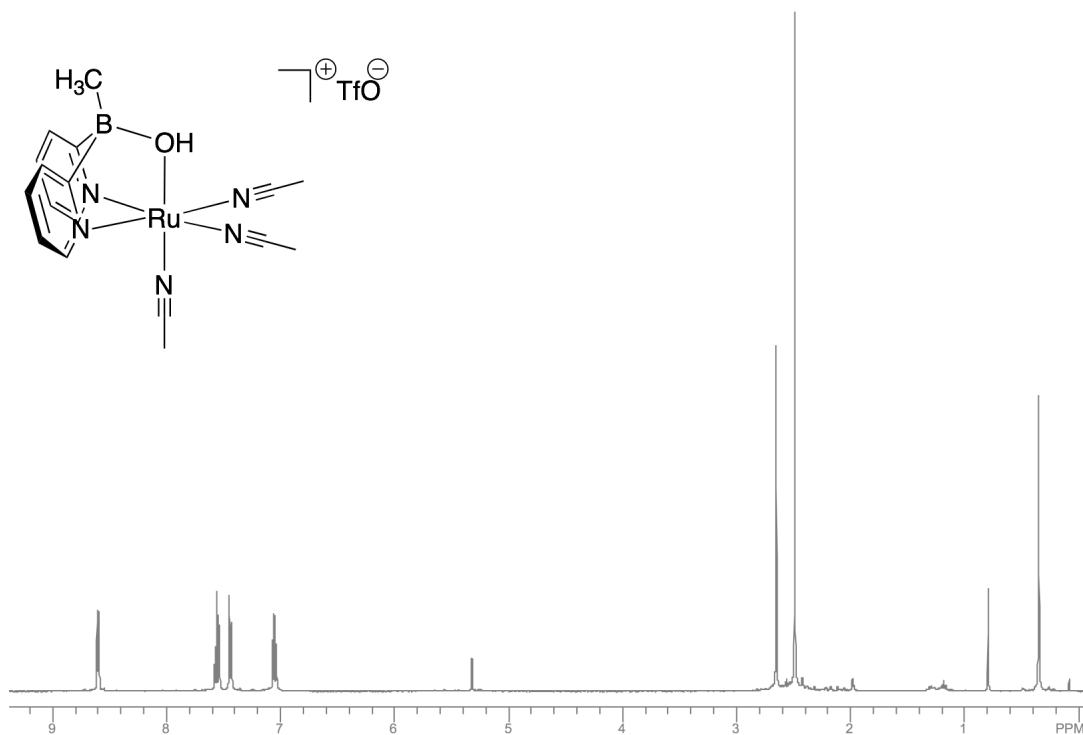


Figure S10. 400 MHz ^1H NMR of Compound **1** in Dichloromethane- d_2 .

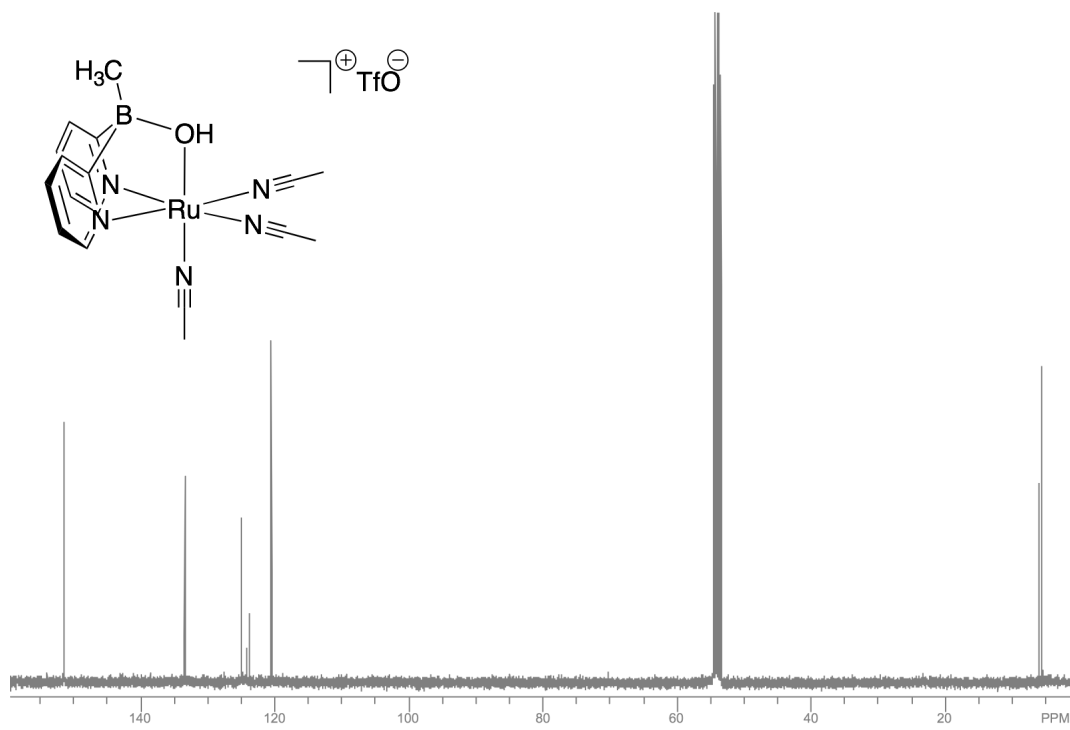


Figure S11. 100 MHz $^{13}\text{C}\{\text{H}^1\}$ NMR spectrum for Compound 1 in Dichloromethane- d_2 .

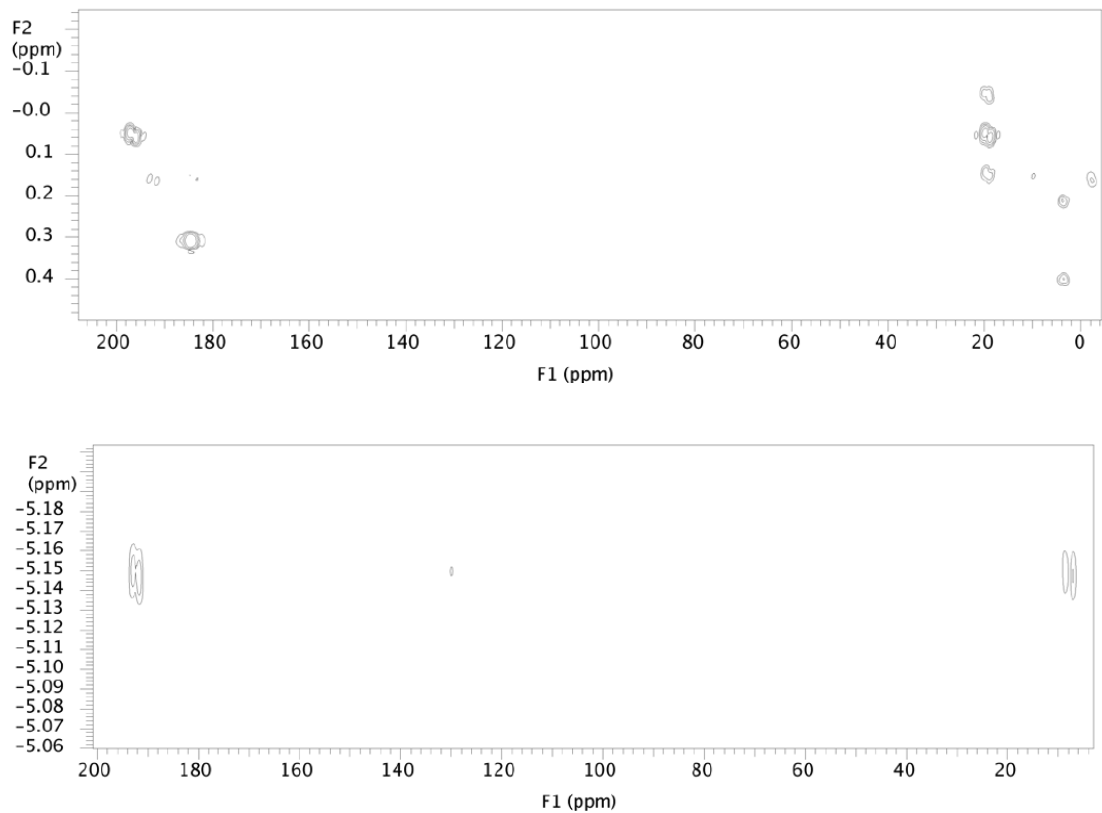


Figure S12. Methyl Region of ^1H - ^{13}C HMBC for **6** and **7** Equilibrating in Acetonitrile- d_3 at 25 °C *Top*: showing no interaction of unbound methyl groups with acetonitrile ligands *Bottom*: showing the interaction of the agostic methyl in **7** with bound acetonitrile.

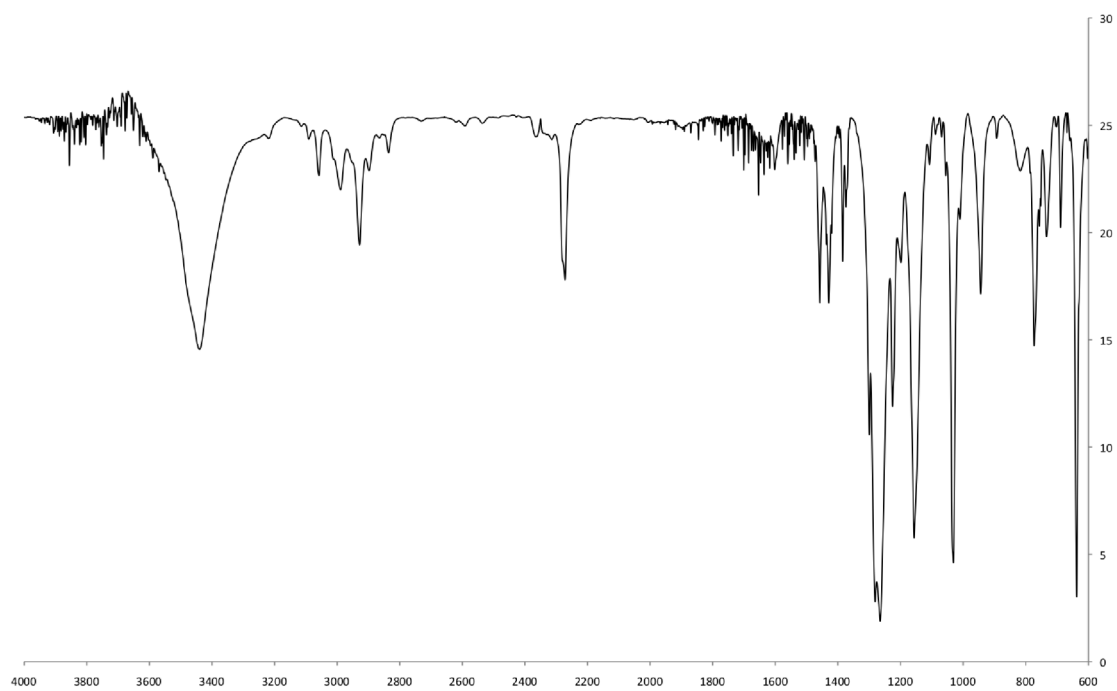


Figure S13. Infrared Spectrum of **1** (KBr pellet).

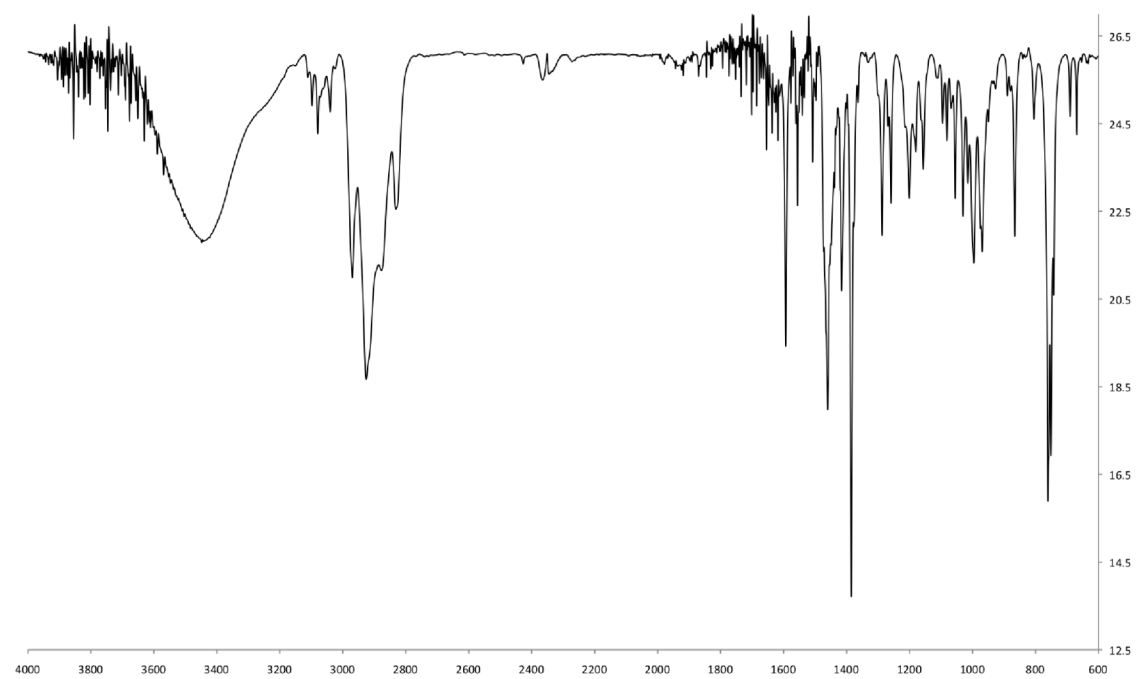


Figure S14. Infrared Spectrum of **4** (KBr pellet).

VI. Oxidation of 1-(4-methoxyphenyl)ethanol with Compound 1

In the glovebox, 1.2 mg **1** (2.1 mmol, 3.3 mol%) was dissolved in 0.70 mL acetone-*d*₆ with 10.0 μ L (71.0 mmol) 1-(4-methoxyphenyl)ethanol and 1.2 mg potassium tert-butoxide (12.6 mmol, 19.8 mol %) in a J. Young NMR tube under nitrogen atmosphere. The tube was heated in a regulated oil-bath at 100 °C for 72 h. Conversion and yield were calculated based on the integration of the *t*-butoxide methyl peaks to the aromatic resonances.

VII. Crystal Structure Data

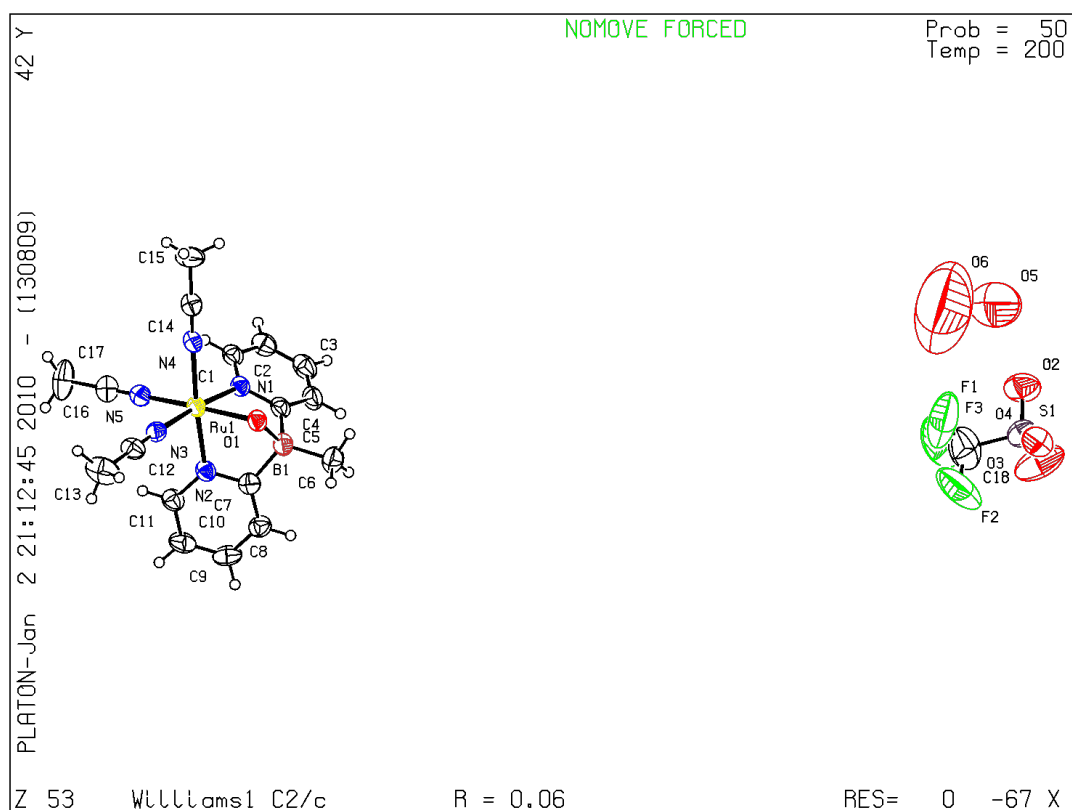


Figure S15. ORTEP diagram of complex **1**. Ellipsoids are drawn at the 50% probability level.

Yellow needles of compound **1** were grown by slow diffusion of diethyl ether into a concentrated, cooled (-40 °C) acetonitrile solution. Diffraction data were collected at 200(2) K on a SMART APEX CCD platform diffractometer with graphite fine-focused monochromatic Mo-K α radiation ($\lambda = 0.71073 \text{ \AA}$). The cell parameters for (C₁₈H₂₀BF₃N₅O₆RuS) were obtained from the least-squares refinement of the spots (from 60 collected frames) using the SMART program on a single crystal sample measuring 0.48 x 0.12 x 0.10 mm³. A hemisphere of data were collected (10 s/frame scan time for a

sphere of diffraction data) up to a resolution of 0.77 Å and the intensity data were processed using the “Saint Plus” program to yield the reflection data file. All calculations for the structure determination were carried out using the SHELXTL package (version 6.14).⁸ Initial position of the ruthenium atom were located by a Patterson function using the program XS. The remaining atoms were located in the difference-Fourier maps, refined on F² by full matrix least squares techniques using SHELX with 5,811 independent reflections within the range of θ 1.5° to 27.56° (completeness 97.2%). Absorption corrections were applied by SADABS,⁹ with an R_(int) = 6.1 %. Calculated hydrogen position were input and refined in a riding manner along with the corresponding carbons. A summary of the refinement details and the resulting factors are given in Table (C₁₈H₂₀BF₃N₅O₆RuS).

Final structure refinement for C₁₈H₂₀BF₃N₅O₆RuS at convergence resulted in R₁ = 5.6 % and wR₂ = 12.4 % for those 5811 data with I > 4 σ . The data to parameter ratio is 18 : 1. The crystal system found is monoclinic, space group C2/c with Z equal to 8 and unit cell dimensions: a = 23.644(8) Å b = 8.032(3) Å, c = 29.052(9) Å.

There are two water molecules located in the crystal lattice in the proximity of the trifluoromethanesulfonate. The triflate anion was located in the asymmetric unit cell and behaved well throughout anisotropic refinement.

Table S5. Crystal Data and Structure Refinement for **1**.

Empirical formula	C ₁₈ H ₂₀ BF ₃ N ₅ O ₆ RuS	
Formula weight	603.33	
Temperature	200(2) K	
Wavelength	0.71073 Å	
Crystal system	Monoclinic	
Space group	C2/c	
Unit cell dimensions	a = 23.644(8) Å	a = 90°.
	b = 8.032(3) Å	b = 110.535(5) °.
	c = 29.052(9) Å	g = 90°.
Volume	5167(3) Å ³	
Z	8	
Density (calculated)	1.551 Mg/m ³	
Absorption coefficient	0.750 mm ⁻¹	
F(000)	2424	
Crystal size	0.48 x 0.12 x 0.10 mm ³	
Theta range for data collection	1.50 to 27.56°.	
Index ranges	-30<=h<=28, -7<=k<=10, -37<=l<=37	
Reflections collected	15109	
Independent reflections	5811 [R(int) = 0.0606]	
Completeness to theta = 27.56°	97.2%	
Absorption correction	Empirical	
Max. and min. transmission	0.9288 and 0.7147	
Refinement method	Full-matrix least-squares on F ²	
Data / restraints / parameters	5811 / 0 / 320	
Goodness-of-fit on F ²	0.984	
Final R indices [I>2sigma(I)]	R1 = 0.0561, wR2 = 0.1236	
R indices (all data)	R1 = 0.1040, wR2 = 0.1421	
Largest diff. peak and hole	0.690 and -0.559 Å ⁻³	

Table S6. Atomic coordinates ($\times 10^4$) and equivalent isotropic displacement parameters ($\text{\AA}^2 \times 10^3$) for $\text{C}_{18}\text{H}_{20}\text{BF}_3\text{N}_5\text{O}_6\text{RuS}$. $U(\text{eq})$ is defined as one third of the trace of the orthogonalized U^{ij} tensor.

	x	y	z	U(eq)
Ru(1)	3215(1)	5806(1)	8947(1)	34(1)
B(1)	3623(3)	4406(7)	8225(2)	41(1)
N(1)	2615(2)	5016(5)	8286(1)	35(1)
N(2)	3593(2)	3491(5)	9034(1)	38(1)
N(3)	3871(2)	6474(5)	9589(2)	38(1)
N(4)	2828(2)	8102(5)	8797(1)	37(1)
N(5)	2686(2)	5359(5)	9339(2)	40(1)
O(1)	3747(1)	6074(4)	8505(1)	38(1)
C(1)	2012(2)	5082(6)	8139(2)	41(1)
C(2)	1647(2)	4486(7)	7693(2)	50(1)
C(3)	1914(3)	3795(7)	7384(2)	54(2)
C(4)	2533(3)	3754(6)	7532(2)	48(1)
C(5)	2888(2)	4393(6)	7982(2)	41(1)
C(6)	3977(3)	4219(8)	7843(2)	59(2)
C(7)	3761(2)	2992(6)	8652(2)	40(1)
C(8)	4014(2)	1429(7)	8666(2)	44(1)
C(9)	4100(2)	386(7)	9057(2)	52(2)
C(10)	3944(2)	930(7)	9453(2)	52(1)
C(11)	3693(2)	2485(6)	9428(2)	44(1)
C(12)	4230(2)	6691(6)	9959(2)	45(1)
C(13)	4698(3)	6966(8)	10438(2)	81(2)
C(14)	2572(2)	9320(7)	8691(2)	42(1)
C(15)	2251(3)	10893(7)	8557(2)	64(2)
C(16)	2411(3)	5201(7)	9585(2)	52(1)
C(17)	2059(3)	5027(10)	9912(2)	90(2)
C(18)	4543(5)	2256(18)	1549(4)	126(4)
F(1)	4525(3)	3771(14)	1736(2)	202(4)
F(2)	5055(3)	1584(11)	1812(2)	195(4)
F(3)	4081(3)	1627(14)	1618(3)	225(4)
S(1)	4463(1)	2433(2)	924(1)	69(1)
O(2)	3911(2)	3322(7)	699(2)	99(2)
O(3)	4430(3)	769(8)	763(3)	145(3)
O(4)	4998(2)	3286(6)	943(2)	79(1)
O(5)	3417(6)	6398(18)	736(5)	301(7)
O(6)	4135(12)	8410(70)	1496(9)	780(40)

Table S7. Bond lengths [Å] and angles [°] for C₁₈H₂₀BF₃N₅O₆RuS.

Ru(1)-N(5)	1.997(4)	C(2)-C(3)	1.381(8)
Ru(1)-N(3)	2.034(4)	C(3)-C(4)	1.374(8)
Ru(1)-N(4)	2.038(4)	C(4)-C(5)	1.382(7)
Ru(1)-N(2)	2.040(4)	C(7)-C(8)	1.385(7)
Ru(1)-N(1)	2.047(4)	C(8)-C(9)	1.370(7)
Ru(1)-O(1)	2.099(3)	C(9)-C(10)	1.394(8)
B(1)-O(1)	1.542(6)	C(10)-C(11)	1.374(7)
B(1)-C(6)	1.614(7)	C(12)-C(13)	1.459(7)
B(1)-C(7)	1.630(8)	C(14)-C(15)	1.455(7)
B(1)-C(5)	1.630(8)	C(16)-C(17)	1.474(8)
N(1)-C(1)	1.339(6)	C(18)-F(3)	1.284(10)
N(1)-C(5)	1.360(6)	C(18)-F(2)	1.300(12)
N(2)-C(11)	1.352(6)	C(18)-F(1)	1.339(14)
N(2)-C(7)	1.363(6)	C(18)-S(1)	1.765(11)
N(3)-C(12)	1.126(6)	S(1)-O(3)	1.409(6)
N(4)-C(14)	1.134(6)	S(1)-O(4)	1.422(4)
N(5)-C(16)	1.129(6)	S(1)-O(2)	1.428(5)
C(1)-C(2)	1.367(7)		

N(5)-Ru(1)-N(3)	87.39(16)	B(1)-O(1)-Ru(1)	101.0(3)
N(5)-Ru(1)-N(4)	87.70(16)	N(1)-C(1)-C(2)	122.4(5)
N(3)-Ru(1)-N(4)	95.68(15)	C(1)-C(2)-C(3)	118.4(5)
N(5)-Ru(1)-N(2)	95.77(16)	C(4)-C(3)-C(2)	119.1(5)
N(3)-Ru(1)-N(2)	88.11(15)	C(3)-C(4)-C(5)	120.9(5)
N(4)-Ru(1)-N(2)	174.98(15)	N(1)-C(5)-C(4)	118.9(5)
N(5)-Ru(1)-N(1)	96.39(16)	N(1)-C(5)-B(1)	113.2(4)
N(3)-Ru(1)-N(1)	174.75(16)	C(4)-C(5)-B(1)	127.8(5)
N(4)-Ru(1)-N(1)	88.13(15)	N(2)-C(7)-C(8)	119.3(5)
N(2)-Ru(1)-N(1)	87.89(15)	N(2)-C(7)-B(1)	112.2(4)
N(5)-Ru(1)-O(1)	174.98(15)	C(8)-C(7)-B(1)	128.5(5)
N(3)-Ru(1)-O(1)	96.09(14)	C(9)-C(8)-C(7)	121.0(5)
N(4)-Ru(1)-O(1)	95.54(14)	C(8)-C(9)-C(10)	119.1(5)
N(2)-Ru(1)-O(1)	80.76(14)	C(11)-C(10)-C(9)	118.5(5)
N(1)-Ru(1)-O(1)	79.91(14)	N(2)-C(11)-C(10)	122.1(5)
O(1)-B(1)-C(6)	113.3(4)	N(3)-C(12)-C(13)	179.8(7)
O(1)-B(1)-C(7)	104.6(4)	N(4)-C(14)-C(15)	179.3(6)
C(6)-B(1)-C(7)	116.4(4)	N(5)-C(16)-C(17)	178.8(6)
O(1)-B(1)-C(5)	102.1(4)	F(3)-C(18)-F(2)	114.4(10)
C(6)-B(1)-C(5)	115.7(4)	F(3)-C(18)-F(1)	98.2(11)
C(7)-B(1)-C(5)	102.9(4)	F(2)-C(18)-F(1)	107.1(11)
C(1)-N(1)-C(5)	120.2(4)	F(3)-C(18)-S(1)	113.7(9)
C(1)-N(1)-Ru(1)	126.7(3)	F(2)-C(18)-S(1)	112.4(9)
C(5)-N(1)-Ru(1)	113.1(3)	F(1)-C(18)-S(1)	109.8(9)
C(11)-N(2)-C(7)	119.9(4)	O(3)-S(1)-O(4)	114.5(4)
C(11)-N(2)-Ru(1)	126.0(3)	O(3)-S(1)-O(2)	112.8(4)
C(7)-N(2)-Ru(1)	114.0(3)	O(4)-S(1)-O(2)	115.7(3)
C(12)-N(3)-Ru(1)	173.3(4)	O(3)-S(1)-C(18)	103.7(6)
C(14)-N(4)-Ru(1)	174.8(4)	O(4)-S(1)-C(18)	103.0(4)
C(16)-N(5)-Ru(1)	174.6(4)	O(2)-S(1)-C(18)	105.3(5)

Table S8. Hydrogen coordinates ($\times 10^4$) and isotropic displacement parameters ($\text{\AA}^2 \times 10^3$) for $\text{C}_{18}\text{H}_{20}\text{BF}_3\text{N}_5\text{O}_6\text{RuS}$.

	x	y	z	U(eq)
H(1)	1831	5561	8353	50
H(2)	1220	4545	7598	59
H(3)	1672	3355	7074	65
H(4)	2719	3278	7321	57
H(6A)	3880	5168	7617	89
H(6B)	3853	3184	7656	89
H(6C)	4413	4191	8025	89
H(8)	4129	1076	8399	53
H(9)	4264	-696	9060	63
H(10)	4009	241	9732	62
H(11)	3586	2866	9697	52
H(13A)	4547	7741	10629	121
H(13B)	5057	7438	10393	121
H(13C)	4802	5904	10614	121
H(15A)	1911	10909	8675	96
H(15B)	2101	11016	8199	96
H(15C)	2527	11813	8707	96
H(17A)	2282	4326	10194	135
H(17B)	1669	4510	9732	135
H(17C)	1993	6128	10030	135

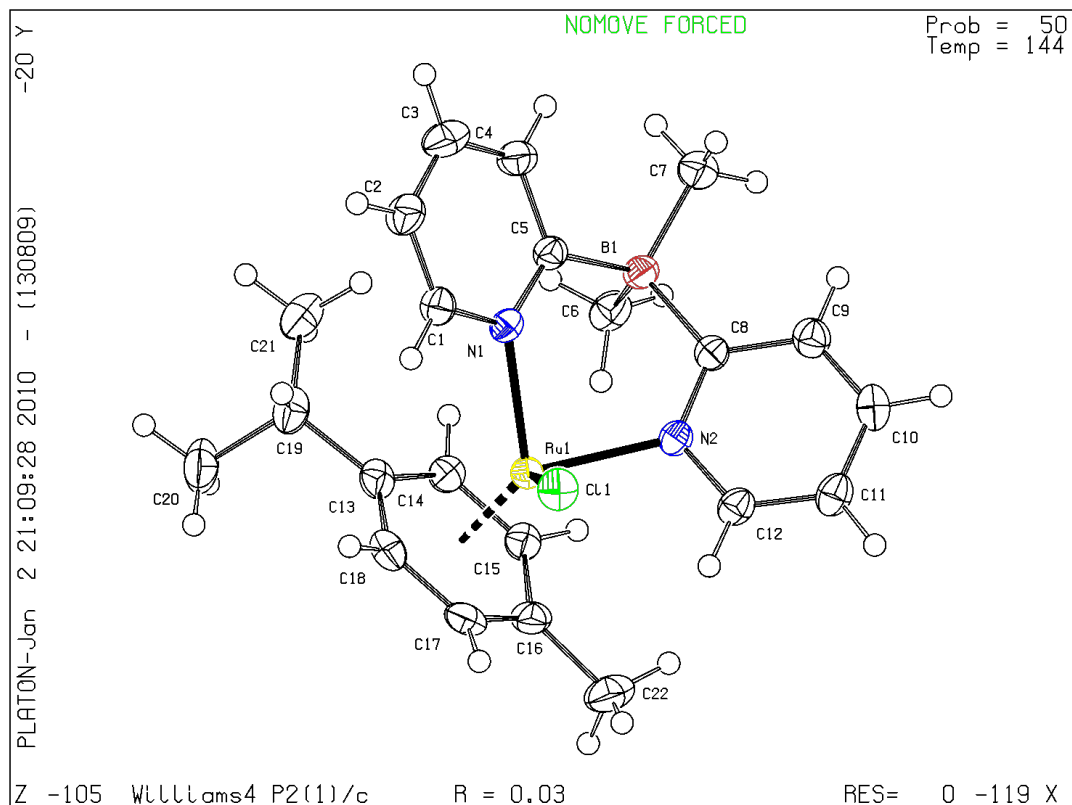


Figure S16. ORTEP diagram of complex **4**. Ellipsoids are drawn at the 50% probability level.

Red blocks of compound **4** (CCDC 738031) were grown by slow diffusion of hexanes into a concentrated, benzene solution. Diffraction data were collected at 144(2) K on a SMART APEX CCD platform diffractometer with graphite fine-focused monochromatic Mo-K α radiation ($\lambda = 0.71073 \text{ \AA}$). The cell parameters for (C₂₂H₂₈BCIN₂Ru) were obtained from the least-squares refinement of the spots (from 60 collected frames) using the SMART program on a single crystal sample measuring 0.51 x 0.14 x 0.01 mm³. A hemisphere of data were collected (10 s/frame scan time for a sphere of diffraction data) up to a resolution of 0.77 \AA and the intensity data were processed using the “Saint Plus” program to yield the reflection data file. All calculations for the structure determination were carried out using the SHELXTL package (version 6.14). Initial position of the ruthenium atom were located by a Patterson function using the program XS. The remaining atoms were located in the difference-Fourier maps, refined on F² by full matrix least squares techniques using SHELX with 5,811 independent reflections within the range of θ 1.5° to 27.56° (completeness 97.6%). Absorption corrections were applied by SADABS, with an R_(int) = 3.1 %. Calculated hydrogen position were input and refined in a riding manner along with the corresponding carbons. A summary of the refinement details and the resulting factors are given in **Table S9** (C₂₂H₂₈BCIN₂Ru).

Final structure refinement for $C_{22}H_{28}BClN_2Ru$ at convergence resulted in $R_1 = 3.2\%$ and $wR_2 = 7.6\%$ for those 4645 data with $I > 4\sigma$. The data to parameter ratio is 19:1. The crystal system found is monoclinic, space group P2(1)/c with Z equal to 4 and unit cell dimensions: $a = 8.988(8) \text{ \AA}$, $b = 13.637(13) \text{ \AA}$, $c = 17.364(16) \text{ \AA}$.

Table S9. Crystal data and structure refinement for $C_{22}H_{28}BClN_2Ru$.

Empirical formula	$C_{22}H_{28}BClN_2Ru$	
Formula weight	467.79	
Temperature	144(2) K	
Wavelength	0.71073 \AA	
Crystal system	Monoclinic	
Space group	P2(1)/c	
Unit cell dimensions	$a = 8.9877(8) \text{ \AA}$	$\alpha = 90^\circ$.
	$b = 13.6367(13) \text{ \AA}$	$\beta = 103.424(2)^\circ$.
	$c = 17.3641(16) \text{ \AA}$	$\gamma = 90^\circ$.
Volume	2070.0(3) \AA^3	
Z	4	
Density (calculated)	1.501 Mg/m^3	
Absorption coefficient	0.895 mm^{-1}	
F(000)	960	
Crystal size	0.51 x 0.14 x 0.01 mm^3	
Theta range for data collection	1.92 to 27.51 $^\circ$.	
Index ranges	-11 $\leq h \leq$ 11, -17 $\leq k \leq$ 17, -22 $\leq l \leq$ 16	
Reflections collected	12497	
Independent reflections	4645 [R(int) = 0.0310]	
Completeness to theta = 27.51 $^\circ$	97.6%	
Absorption correction	Semi-empirical	
Max. and min. transmission	0.9938 and 0.6600	
Refinement method	Full-matrix least-squares on F^2	
Data / restraints / parameters	4645 / 0 / 249	
Goodness-of-fit on F^2	1.058	
Final R indices [$I > 2\sigma(I)$]	R1 = 0.0322, wR2 = 0.0760	
R indices (all data)	R1 = 0.0421, wR2 = 0.0800	
Largest diff. peak and hole	0.931 and -0.281 e.\AA^{-3}	

Table S10. Bond lengths [\AA] and angles [$^\circ$] for $\text{C}_{22}\text{H}_{28}\text{BClN}_2\text{Ru}$.

Ru(1)-N(1)	2.0982(19)	C(2)-C(3)	1.384(4)
Ru(1)-N(2)	2.117(2)	C(3)-C(4)	1.371(4)
Ru(1)-C(15)	2.185(2)	C(4)-C(5)	1.412(3)
Ru(1)-C(14)	2.191(2)	C(8)-C(9)	1.401(3)
Ru(1)-C(17)	2.194(2)	C(9)-C(10)	1.379(4)
Ru(1)-C(18)	2.200(2)	C(10)-C(11)	1.383(4)
Ru(1)-C(13)	2.240(2)	C(11)-C(12)	1.370(4)
Ru(1)-C(16)	2.247(2)	C(13)-C(18)	1.396(3)
Ru(1)-Cl(1)	2.4212(6)	C(13)-C(14)	1.422(3)
B(1)-C(7)	1.634(4)	C(13)-C(19)	1.523(3)
B(1)-C(5)	1.636(4)	C(14)-C(15)	1.409(3)
B(1)-C(8)	1.644(4)	C(15)-C(16)	1.427(3)
B(1)-C(6)	1.656(4)	C(16)-C(17)	1.386(4)
N(1)-C(1)	1.352(3)	C(16)-C(22)	1.513(3)
N(1)-C(5)	1.361(3)	C(17)-C(18)	1.433(3)
N(2)-C(12)	1.353(3)	C(19)-C(21)	1.534(4)
N(2)-C(8)	1.362(3)	C(19)-C(20)	1.533(4)
C(1)-C(2)	1.370(3)		

N(1)-Ru(1)-N(2)	85.60(8)	C(12)-N(2)-C(8)	120.2(2)
N(1)-Ru(1)-C(15)	126.59(8)	C(12)-N(2)-Ru(1)	114.88(16)
N(2)-Ru(1)-C(15)	93.88(9)	C(8)-N(2)-Ru(1)	124.88(15)
N(1)-Ru(1)-C(14)	96.24(8)	N(1)-C(1)-C(2)	123.2(2)
N(2)-Ru(1)-C(14)	116.09(9)	C(1)-C(2)-C(3)	117.9(2)
C(15)-Ru(1)-C(14)	37.57(9)	C(4)-C(3)-C(2)	118.8(2)
N(1)-Ru(1)-C(17)	147.19(9)	C(3)-C(4)-C(5)	122.7(3)
N(2)-Ru(1)-C(17)	125.81(9)	N(1)-C(5)-C(4)	116.5(2)
C(15)-Ru(1)-C(17)	66.65(10)	N(1)-C(5)-B(1)	122.5(2)
C(14)-Ru(1)-C(17)	79.18(9)	C(4)-C(5)-B(1)	121.0(2)
N(1)-Ru(1)-C(18)	110.21(9)	N(2)-C(8)-C(9)	117.4(2)
N(2)-Ru(1)-C(18)	163.86(9)	N(2)-C(8)-B(1)	121.2(2)
C(15)-Ru(1)-C(18)	79.47(10)	C(9)-C(8)-B(1)	121.4(2)
C(14)-Ru(1)-C(18)	66.79(10)	C(10)-C(9)-C(8)	122.5(3)
C(17)-Ru(1)-C(18)	38.05(9)	C(9)-C(10)-C(11)	118.3(2)
N(1)-Ru(1)-C(13)	89.27(8)	C(12)-C(11)-C(10)	118.4(2)
N(2)-Ru(1)-C(13)	152.19(9)	N(2)-C(12)-C(11)	123.2(2)
C(15)-Ru(1)-C(13)	67.62(9)	C(18)-C(13)-C(14)	118.1(2)
C(14)-Ru(1)-C(13)	37.43(9)	C(18)-C(13)-C(19)	118.7(2)
C(17)-Ru(1)-C(13)	67.27(10)	C(14)-C(13)-C(19)	123.2(2)
C(18)-Ru(1)-C(13)	36.63(9)	C(18)-C(13)-Ru(1)	70.15(14)
N(1)-Ru(1)-C(16)	163.51(8)	C(14)-C(13)-Ru(1)	69.41(14)
N(2)-Ru(1)-C(16)	98.54(9)	C(19)-C(13)-Ru(1)	132.38(17)
C(15)-Ru(1)-C(16)	37.54(9)	C(15)-C(14)-C(13)	120.9(2)
C(14)-Ru(1)-C(16)	67.57(9)	C(15)-C(14)-Ru(1)	71.01(13)
C(17)-Ru(1)-C(16)	36.34(10)	C(13)-C(14)-Ru(1)	73.16(14)
C(18)-Ru(1)-C(16)	67.25(10)	C(14)-C(15)-C(16)	120.9(2)
C(13)-Ru(1)-C(16)	79.62(9)	C(14)-C(15)-Ru(1)	71.43(13)
N(1)-Ru(1)-Cl(1)	85.67(5)	C(16)-C(15)-Ru(1)	73.56(14)
N(2)-Ru(1)-Cl(1)	84.81(5)	C(17)-C(16)-C(15)	117.6(2)
C(15)-Ru(1)-Cl(1)	147.59(7)	C(17)-C(16)-C(22)	121.9(2)
C(14)-Ru(1)-Cl(1)	159.09(7)	C(15)-C(16)-C(22)	120.5(3)
C(17)-Ru(1)-Cl(1)	87.94(7)	C(17)-C(16)-Ru(1)	69.78(14)
C(18)-Ru(1)-Cl(1)	92.95(7)	C(15)-C(16)-Ru(1)	68.90(14)
C(13)-Ru(1)-Cl(1)	122.07(7)	C(22)-C(16)-Ru(1)	132.71(19)
C(16)-Ru(1)-Cl(1)	110.53(7)	C(16)-C(17)-C(18)	121.8(2)
C(7)-B(1)-C(5)	108.8(2)	C(16)-C(17)-Ru(1)	73.88(15)
C(7)-B(1)-C(8)	111.4(2)	C(18)-C(17)-Ru(1)	71.20(14)
C(5)-B(1)-C(8)	107.5(2)	C(13)-C(18)-C(17)	120.5(2)
C(7)-B(1)-C(6)	105.6(2)	C(13)-C(18)-Ru(1)	73.22(14)
C(5)-B(1)-C(6)	114.9(2)	C(17)-C(18)-Ru(1)	70.74(14)
C(8)-B(1)-C(6)	108.8(2)	C(13)-C(19)-C(21)	114.9(2)
C(1)-N(1)-C(5)	120.9(2)	C(13)-C(19)-C(20)	107.7(2)
C(1)-N(1)-Ru(1)	114.89(16)	C(21)-C(19)-C(20)	110.4(2)
C(5)-N(1)-Ru(1)	123.89(16)		

Table S11. Atomic coordinates ($\times 10^4$) and equivalent isotropic displacement parameters ($\text{\AA}^2 \times 10^3$) for $\text{C}_{22}\text{H}_{28}\text{BClN}_2\text{Ru}$. $U(\text{eq})$ is defined as one third of the trace of the orthogonalized U^{ij} tensor.

	x	y	z	U(eq)
Ru(1)	5956(1)	3974(1)	1771(1)	20(1)
B(1)	9390(3)	4488(2)	3072(2)	26(1)
Cl(1)	4522(1)	5457(1)	1340(1)	30(1)
N(1)	7862(2)	4757(1)	1600(1)	22(1)
N(2)	6423(2)	4632(1)	2906(1)	23(1)
C(1)	7720(3)	5123(2)	863(2)	26(1)
C(2)	8910(3)	5540(2)	610(2)	33(1)
C(3)	10319(3)	5588(2)	1141(2)	38(1)
C(4)	10452(3)	5239(2)	1894(2)	31(1)
C(5)	9213(3)	4819(2)	2149(2)	24(1)
C(6)	9605(3)	3295(2)	3237(2)	33(1)
C(7)	10928(3)	4997(2)	3611(2)	38(1)
C(8)	7846(3)	4856(2)	3343(1)	24(1)
C(9)	7942(3)	5385(2)	4044(2)	30(1)
C(10)	6667(3)	5640(2)	4314(2)	32(1)
C(11)	5246(3)	5365(2)	3869(2)	30(1)
C(12)	5171(3)	4879(2)	3171(2)	27(1)
C(13)	6378(3)	2841(2)	912(2)	27(1)
C(14)	6925(3)	2511(2)	1705(2)	26(1)
C(15)	5954(3)	2484(2)	2235(2)	26(1)
C(16)	4389(3)	2775(2)	1989(2)	30(1)
C(17)	3891(3)	3139(2)	1228(2)	31(1)
C(18)	4871(3)	3174(2)	685(2)	30(1)
C(19)	7355(3)	2844(2)	303(2)	34(1)
C(20)	6850(4)	1974(2)	-256(2)	47(1)
C(21)	9086(3)	2806(2)	653(2)	39(1)
C(22)	3331(3)	2685(2)	2548(2)	43(1)

Table S12. Hydrogen coordinates ($\times 10^4$) and isotropic displacement parameters ($\text{\AA}^2 \times 10^3$) for $\text{C}_{22}\text{H}_{28}\text{BClN}_2\text{Ru}$.

	x	y	z	U(eq)
H(1)	6748	5090	503	31
H(2)	8772	5788	87	39
H(3)	11179	5859	986	46
H(4)	11417	5282	2260	37
H(6A)	10229	3019	2896	49
H(6B)	8599	2977	3119	49
H(6C)	10113	3182	3793	49
H(7A)	11833	4727	3463	56
H(7B)	10988	4861	4172	56
H(7C)	10887	5707	3523	56
H(9)	8922	5575	4346	36
H(10)	6763	5995	4794	38
H(11)	4343	5511	4042	36
H(12)	4193	4706	2857	33
H(14)	8049	2410	1913	31
H(15)	6405	2363	2810	32
H(17)	2888	3492	1087	37
H(18)	4533	3543	177	35
H(19)	7125	3460	-15	41
H(20A)	7064	1360	42	71
H(20B)	7412	1984	-676	71
H(20C)	5750	2023	-491	71
H(21A)	9352	2184	934	59
H(21B)	9386	3352	1023	59
H(21C)	9627	2858	225	59
H(22A)	2471	3140	2384	64
H(22B)	3894	2847	3088	64
H(22C)	2944	2012	2536	64

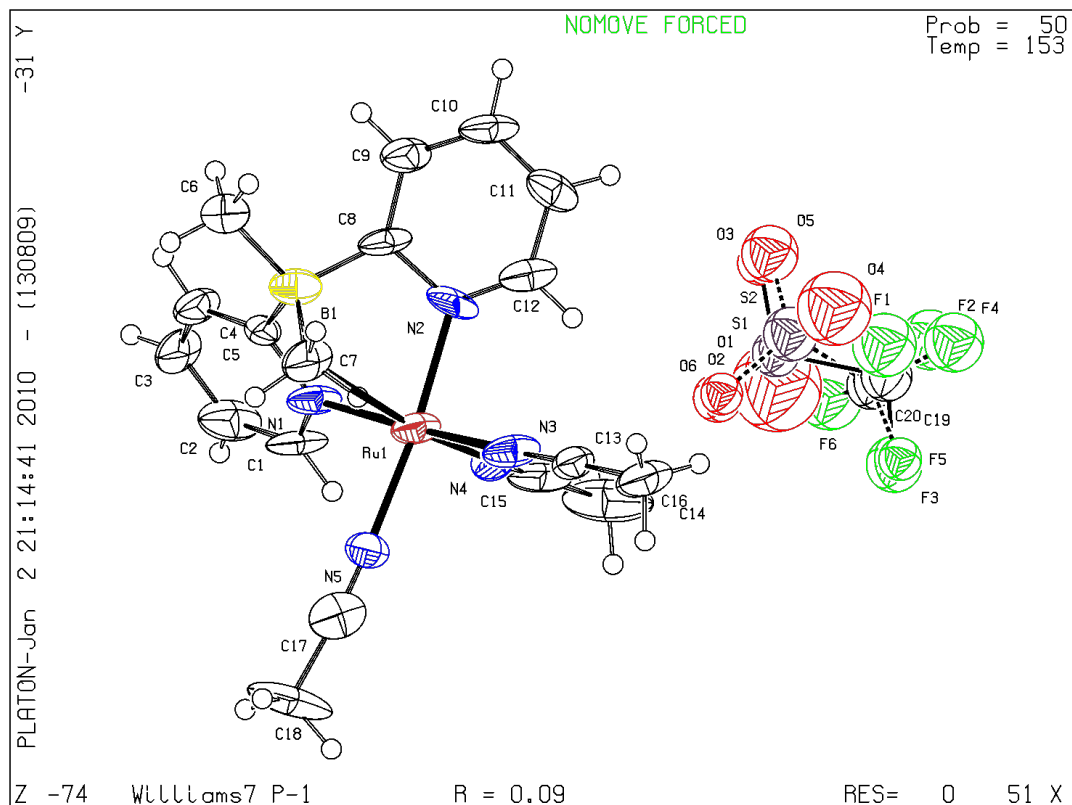


Figure S17. ORTEP diagram of complex **7**. Ellipsoids are drawn at the 50% probability level.

Small orange needles of compound **7** were grown by slow diffusion of hexanes into a concentrated, cooled ($-40\text{ }^{\circ}\text{C}$) dichloromethane solution. Diffraction data were collected at $153(2)\text{ K}$ on a SMART APEX CCD platform diffractometer with graphite fine-focused monochromatic $\text{Mo-K}\alpha$ radiation ($\lambda = 0.71073\text{ \AA}$). The cell parameters for ($\text{C}_{19}\text{H}_{22}\text{BF}_3\text{N}_5\text{O}_3\text{RuS}$) were obtained from the least-squares refinement of the spots using the SMART program on a single crystal sample measuring $0.08 \times 0.04 \times 0.04\text{ mm}^3$. A hemisphere of data were collected (10 s/frame scan time for a sphere of diffraction data) up to a resolution of 0.77 \AA and the intensity data were processed using the “Saint Plus” program to yield the reflection data file. All calculations for the structure determination were carried out using the SHELXTL package (version 6.14). Initial position of the ruthenium atom were located by a Patterson function using the program XS. The remaining atoms were located in the difference-Fourier maps, refined on F^2 by full matrix least squares techniques using SHELX with 5724 independent reflections within the range of $\theta\ 1.30^{\circ}$ to 28.40° (completeness 78.4%). Absorption corrections were applied by SADABS. Calculated hydrogen position were input and refined in a riding manner along with the corresponding carbons. A summary of the refinement details and the resulting factors are given in **Table S13** ($\text{C}_{19}\text{H}_{22}\text{BF}_3\text{N}_5\text{O}_3\text{RuS}$).

Final structure refinement for $C_{19}H_{22}BF_3N_5O_3RuS$ at convergence resulted in $R_1 = 9.2\%$ and $wR_2 = 18.9\%$ for those data with $I > 4\sigma$. The data to parameter ratio is 15.8:1. The crystal system found is triclinic, space group P-1 with Z equal to 2 and unit cell dimensions: $a = 8.055(16) \text{ \AA}$, $b = 9.457(18) \text{ \AA}$, $c = 15.79(3) \text{ \AA}$.

Because of the transient nature of **7**, it was difficult to form and preserve large crystals of this compound throughout the mounting and data acquisition process. Thus, the quantity of data collected for this sample is less good than for **1** and **4**. Fortunately, all atoms in the metal cation fragment were accurately located and refined. We found, however, that the triflate anion is highly disordered. This was modeled as two separate partially-occupied triflates with isotropic atoms.

Table S13. Crystal data and structure refinement for **7**.

Empirical formula	$C_{19}H_{22}BF_3N_5O_3RuS$	
Formula weight	569.36	
Temperature	153(2) K	
Wavelength	0.71073 \AA	
Crystal system	Triclinic	
Space group	P-1	
Unit cell dimensions	$a = 8.055(16) \text{ \AA}$	$\alpha = 96.57(4)^\circ$.
	$b = 9.457(18) \text{ \AA}$	$\beta = 91.22(4)^\circ$.
	$c = 15.79(3) \text{ \AA}$	$\gamma = 95.44(3)^\circ$.
Volume	1189(4) \AA^3	
Z	2	
Density (calculated)	1.590 Mg/m^3	
Absorption coefficient	0.801 mm^{-1}	
F(000)	576	
Crystal size	0.08 x 0.04 x 0.04 mm^3	
Theta range for data collection	1.30 to 28.40 $^\circ$.	
Index ranges	-8 $\leq h \leq$ 10, -12 $\leq k \leq$ 6, -15 $\leq l \leq$ 20	
Reflections collected	5724	
Independent reflections	4685 [R(int) = 0.0819]	
Completeness to theta = 28.40 $^\circ$	78.4 %	
Absorption correction	Semi-empirical	
Refinement method	Full-matrix least-squares on F^2	
Data / restraints / parameters	4685 / 34 / 296	
Goodness-of-fit on F^2	1.059	
Final R indices [$I > 2\sigma(I)$]	R1 = 0.0921, wR2 = 0.1887	
R indices (all data)	R1 = 0.2026, wR2 = 0.2468	
Largest diff. peak and hole	1.026 and -1.578 $e.\text{\AA}^{-3}$	

Table S14. Atomic coordinates ($\times 10^4$) and equivalent isotropic displacement parameters ($\text{\AA}^2 \times 10^3$) for **7**. U(eq) is defined as one third of the trace of the orthogonalized U^{ij} tensor.

	x	y	z	U(eq)
B(1)	6730(20)	7725(18)	9496(10)	46(4)
C(1)	6213(16)	9860(15)	7737(9)	55(5)
C(2)	6968(19)	11217(15)	7997(10)	66(5)
C(3)	7680(20)	11505(14)	8799(10)	62(5)
C(4)	7654(18)	10443(14)	9291(9)	52(4)
C(5)	6858(16)	9085(13)	9041(8)	39(4)
C(6)	7319(19)	8122(16)	10504(8)	61(5)
C(7)	4772(18)	6986(14)	9447(9)	60(5)
C(8)	7879(17)	6631(13)	9058(9)	50(4)
C(9)	9422(19)	6270(14)	9307(10)	58(5)
C(10)	10286(18)	5330(15)	8801(10)	54(4)
C(11)	9636(17)	4787(14)	8006(10)	51(4)
C(12)	8116(17)	5192(15)	7787(9)	46(4)
C(13)	3658(16)	3553(15)	7330(8)	40(4)
C(14)	2972(18)	2091(15)	7098(9)	62(5)
C(15)	6253(18)	6713(17)	6038(12)	58(5)
C(16)	6840(20)	6580(20)	5109(11)	104(8)
C(17)	1740(20)	8029(16)	7503(9)	58(5)
C(18)	89(17)	8685(17)	7459(11)	93(7)
N(1)	6152(13)	8812(11)	8229(7)	47(3)
N(2)	7289(14)	6062(11)	8224(8)	47(3)
N(3)	4116(13)	4737(12)	7567(7)	48(4)
N(4)	5803(14)	6747(12)	6708(7)	38(3)
N(5)	2953(14)	7578(11)	7597(7)	43(3)
Ru(1)	5127(2)	6767(1)	7852(1)	43(1)
C(19)	7570(40)	820(40)	4940(20)	64(9)
F(1)	7230(30)	20(20)	5514(16)	100(8)
F(2)	9100(30)	940(30)	4435(12)	89(7)
F(3)	6530(30)	1230(20)	4276(13)	78(7)
S(1)	8086(10)	2629(10)	5542(5)	55(3)
O(1)	8450(60)	3520(50)	4930(30)	200(20)
O(2)	6800(30)	3100(20)	5894(13)	59(6)
O(3)	9500(30)	2660(20)	6092(13)	48(6)
C(20)	7920(50)	1540(40)	4730(20)	58(10)
F(4)	8540(30)	100(30)	4553(14)	86(8)
F(5)	6200(20)	750(20)	4474(12)	45(5)
F(6)	8510(30)	2930(30)	4494(18)	105(9)
O(4)	7470(50)	400(40)	6120(30)	136(14)
O(5)	9290(40)	2150(30)	6261(18)	79(10)
O(6)	6370(30)	2580(20)	6134(13)	43(6)
S(2)	7807(14)	1821(14)	5850(7)	72(4)

Table S15. Bond lengths [Å] and angles [°] for **7**.

B(1)-C(5)	1.540(19)	C(17)-C(18)	1.52(2)
B(1)-C(8)	1.56(2)	N(1)-Ru(1)	2.047(11)
B(1)-C(6)	1.641(19)	N(2)-Ru(1)	2.022(10)
B(1)-C(7)	1.66(2)	N(3)-Ru(1)	2.010(12)
C(1)-N(1)	1.325(15)	N(4)-Ru(1)	1.896(12)
C(1)-C(2)	1.381(18)	N(5)-Ru(1)	2.028(11)
C(2)-C(3)	1.369(16)	C(19)-F(1)	1.26(4)
C(3)-C(4)	1.337(17)	C(19)-F(3)	1.44(4)
C(4)-C(5)	1.390(17)	C(19)-F(2)	1.49(4)
C(5)-N(1)	1.377(13)	C(19)-S(1)	1.87(4)
C(8)-C(9)	1.381(17)	S(1)-O(2)	1.28(2)
C(8)-N(2)	1.419(15)	S(1)-O(1)	1.37(5)
C(9)-C(10)	1.38(2)	S(1)-O(3)	1.412(19)
C(10)-C(11)	1.373(17)	C(20)-F(6)	1.45(4)
C(11)-C(12)	1.366(17)	C(20)-F(4)	1.49(5)
C(12)-N(2)	1.262(18)	C(20)-F(5)	1.54(4)
C(13)-N(3)	1.162(15)	C(20)-S(2)	1.76(4)
C(13)-C(14)	1.442(18)	O(4)-S(2)	1.46(4)
C(15)-N(4)	1.124(19)	O(5)-S(2)	1.34(3)
C(15)-C(16)	1.54(2)	O(6)-S(2)	1.47(2)
C(17)-N(5)	1.116(17)		

C(5)-B(1)-C(8)	109.7(13)	N(4)-Ru(1)-N(2)	92.1(5)
C(5)-B(1)-C(6)	110.3(13)	N(3)-Ru(1)-N(2)	90.2(4)
C(8)-B(1)-C(6)	109.3(11)	N(4)-Ru(1)-N(5)	92.8(5)
C(5)-B(1)-C(7)	109.9(11)	N(3)-Ru(1)-N(5)	92.8(4)
C(8)-B(1)-C(7)	109.3(13)	N(2)-Ru(1)-N(5)	174.3(5)
C(6)-B(1)-C(7)	108.4(13)	N(4)-Ru(1)-N(1)	94.9(5)
N(1)-C(1)-C(2)	123.0(13)	N(3)-Ru(1)-N(1)	176.0(5)
C(3)-C(2)-C(1)	118.9(13)	N(2)-Ru(1)-N(1)	88.4(4)
C(4)-C(3)-C(2)	118.2(13)	N(5)-Ru(1)-N(1)	88.3(4)
C(3)-C(4)-C(5)	123.1(12)	F(1)-C(19)-F(3)	131(3)
N(1)-C(5)-C(4)	117.9(11)	F(1)-C(19)-F(2)	128(3)
N(1)-C(5)-B(1)	111.2(11)	F(3)-C(19)-F(2)	93(2)
C(4)-C(5)-B(1)	130.7(12)	F(1)-C(19)-S(1)	104(2)
C(9)-C(8)-N(2)	116.2(15)	F(3)-C(19)-S(1)	98(2)
C(9)-C(8)-B(1)	130.8(13)	F(2)-C(19)-S(1)	92(2)
N(2)-C(8)-B(1)	112.5(10)	O(2)-S(1)-O(1)	104(2)
C(10)-C(9)-C(8)	122.0(14)	O(2)-S(1)-O(3)	115.2(13)
C(11)-C(10)-C(9)	119.1(12)	O(1)-S(1)-O(3)	109(2)
C(10)-C(11)-C(12)	116.5(15)	O(2)-S(1)-C(19)	111.1(16)
N(2)-C(12)-C(11)	126.5(14)	O(1)-S(1)-C(19)	105(2)
N(3)-C(13)-C(14)	174.5(17)	O(3)-S(1)-C(19)	111.3(14)
N(4)-C(15)-C(16)	176.9(18)	F(6)-C(20)-F(4)	132(4)
N(5)-C(17)-C(18)	174.9(18)	F(6)-C(20)-F(5)	124(3)
C(1)-N(1)-C(5)	118.8(11)	F(4)-C(20)-F(5)	85(2)
C(1)-N(1)-Ru(1)	124.2(9)	F(6)-C(20)-S(2)	104(3)
C(5)-N(1)-Ru(1)	116.9(8)	F(4)-C(20)-S(2)	105(2)
C(12)-N(2)-C(8)	119.4(11)	F(5)-C(20)-S(2)	102(3)
C(12)-N(2)-Ru(1)	126.0(10)	O(5)-S(2)-O(4)	97(2)
C(8)-N(2)-Ru(1)	114.6(9)	O(5)-S(2)-O(6)	119.9(17)
C(13)-N(3)-Ru(1)	172.3(13)	O(4)-S(2)-O(6)	105(2)
C(15)-N(4)-Ru(1)	177.5(12)	O(5)-S(2)-C(20)	114(2)
C(17)-N(5)-Ru(1)	176.2(14)	O(4)-S(2)-C(20)	105(2)
N(4)-Ru(1)-N(3)	88.8(5)	O(6)-S(2)-C(20)	113.0(15)

Table S16. Anisotropic displacement parameters ($\text{\AA}^2 \times 10^3$) for **7**. The anisotropic displacement factor exponent takes the form: $-2 \pi^2 [h^2 a^{*2} U^{11} + \dots + 2 h k a^* b^* U^{12}]$

	U ¹¹	U ²²	U ³³	U ²³	U ¹³	U ¹²
B(1)	42(9)	53(10)	47(10)	23(8)	-6(8)	4(7)
C(1)	34(8)	61(10)	70(10)	30(8)	-32(8)	-8(7)
C(2)	58(11)	47(9)	97(12)	36(10)	-23(10)	-3(8)
C(3)	77(12)	23(8)	79(12)	-5(8)	-37(10)	-7(7)
C(4)	59(10)	32(8)	61(10)	2(7)	-32(8)	-3(7)
C(5)	42(8)	26(7)	49(8)	-1(7)	-19(7)	13(6)
C(6)	56(10)	65(11)	62(11)	0(9)	-18(9)	16(9)
C(7)	74(9)	26(8)	78(11)	6(8)	-36(9)	-6(7)
C(8)	52(8)	23(7)	73(10)	19(7)	-44(7)	-10(6)
C(9)	62(10)	28(9)	83(11)	8(8)	-40(9)	2(7)
C(10)	37(8)	41(9)	86(12)	26(8)	-35(8)	-12(6)
C(11)	38(8)	31(8)	88(11)	22(8)	0(8)	6(6)
C(12)	40(8)	40(9)	59(9)	32(7)	-22(7)	-17(6)
C(13)	39(8)	34(9)	46(9)	3(8)	-17(7)	0(7)
C(14)	60(11)	53(10)	69(11)	12(9)	-36(9)	-7(8)
C(15)	26(8)	67(11)	84(13)	33(11)	-23(9)	-7(7)
C(16)	39(10)	190(20)	102(15)	83(15)	4(10)	11(12)
C(17)	60(11)	53(11)	61(11)	25(9)	-7(9)	-12(9)
C(18)	27(9)	78(13)	190(20)	76(13)	-23(11)	2(9)
N(1)	31(6)	36(7)	72(8)	20(6)	-27(6)	-11(5)
N(2)	36(7)	21(6)	89(9)	25(6)	-15(6)	8(5)
N(3)	33(7)	46(8)	64(9)	26(7)	-21(6)	-16(6)
N(4)	47(7)	37(7)	32(7)	14(6)	-3(6)	-1(6)
N(5)	35(7)	34(7)	59(8)	6(6)	-10(6)	4(5)
Ru(1)	35(1)	38(1)	56(1)	13(1)	-21(1)	-6(1)

Table S17. Hydrogen coordinates ($\times 10^4$) and isotropic displacement parameters ($\text{\AA}^2 \times 10^3$) for **7**.

	x	y	z	U(eq)
H(1)	5714	9668	7180	66
H(2)	6989	11939	7624	79
H(3)	8191	12434	9001	74
H(4)	8201	10624	9837	62
H(6A)	7297	7243	10779	92
H(6B)	6556	8756	10790	92
H(6C)	8455	8605	10546	92
H(7A)	4024	7724	9610	91
H(7B)	4652	6253	9838	91
H(7C)	4483	6547	8864	91
H(9)	9902	6684	9844	70
H(10)	11319	5059	8998	65
H(11)	10213	4164	7628	61
H(12)	7633	4776	7251	55
H(14A)	2940	1584	7606	92
H(14B)	3672	1621	6673	92
H(14C)	1838	2076	6857	92
H(16A)	7211	5630	4958	156
H(16B)	7758	7314	5054	156
H(16C)	5905	6711	4724	156
H(18A)	-529	8285	6931	140
H(18B)	305	9724	7469	140
H(18C)	-572	8468	7950	140

Table S18. Anisotropic displacement parameters ($\text{\AA}^2 \times 10^3$) for **7**. The anisotropic displacement factor exponent takes the form: $-2 \pi^2 [h^2 a^{*2} U^{11} + \dots + 2 h k a^* b^* U^{12}]$

	U ¹¹	U ²²	U ³³	U ²³	U ¹³	U ¹²
B(1)	45(8)	59(10)	32(8)	24(7)	16(6)	14(7)
C(1)	36(7)	58(9)	78(11)	23(8)	-33(7)	-8(6)
C(2)	66(10)	45(8)	103(14)	34(9)	-40(9)	-8(7)
C(3)	80(11)	26(7)	97(13)	12(8)	-42(10)	-8(7)
C(4)	55(8)	34(7)	87(12)	-1(8)	-39(8)	1(6)
C(5)	55(8)	27(7)	83(11)	6(7)	-29(8)	12(6)
C(6)	64(9)	54(9)	76(11)	10(8)	-18(8)	15(7)
C(7)	78(11)	31(7)	115(15)	11(8)	-54(11)	-1(7)
C(8)	47(7)	33(7)	79(11)	20(7)	-49(8)	-9(5)
C(9)	51(8)	33(7)	90(12)	7(8)	-31(8)	-2(6)
C(10)	39(7)	48(8)	98(12)	46(9)	-30(8)	-15(6)
C(11)	44(8)	42(8)	84(11)	23(8)	-16(8)	0(6)
C(12)	36(7)	39(7)	72(10)	26(7)	-23(7)	-14(6)
C(13)	40(7)	41(8)	54(9)	7(7)	-17(6)	2(6)
C(14)	63(9)	41(8)	58(9)	11(7)	-25(7)	-17(6)
C(15)	35(8)	77(11)	82(12)	28(10)	-33(9)	-7(7)
C(16)	54(10)	180(20)	65(12)	69(13)	1(9)	13(11)
C(17)	50(9)	46(8)	84(12)	23(8)	-10(8)	-13(7)
C(18)	26(7)	103(13)	159(18)	80(13)	-11(9)	1(8)
C(19)	98(17)	200(30)	95(18)	-40(19)	-51(14)	66(19)
F(1)	142(12)	300(20)	102(10)	-26(11)	-17(9)	149(14)
F(2)	93(8)	121(9)	97(8)	-13(7)	-47(7)	20(6)
F(3)	198(18)	106(12)	390(30)	76(16)	-16(19)	7(11)
N(1)	38(6)	37(6)	67(8)	9(6)	-29(6)	-2(4)
N(2)	27(5)	29(5)	88(9)	33(6)	-2(6)	6(4)
N(3)	37(6)	39(6)	76(9)	8(6)	-24(6)	-7(5)
N(4)	55(7)	57(7)	27(6)	7(6)	-15(6)	-1(5)
N(5)	28(6)	42(6)	85(9)	10(6)	-13(6)	-4(5)
O(1)	280(30)	183(19)	153(17)	121(14)	8(17)	15(17)
O(2)	64(7)	109(9)	87(9)	9(7)	-41(7)	-1(6)
O(3)	96(10)	124(11)	111(11)	-68(9)	-63(9)	60(8)
Ru(1)	39(1)	38(1)	63(1)	14(1)	-23(1)	-7(1)
S(1)	80(4)	286(11)	178(8)	-154(8)	-77(5)	65(6)

Table S19. Hydrogen coordinates ($\times 10^4$) and isotropic displacement parameters ($\text{\AA}^2 \times 10^3$) for **7**.

	x	y	z	U(eq)
H(1)	5726	9634	7149	69
H(2)	7009	11908	7580	85
H(3)	8208	12434	8960	82
H(4)	8192	10623	9826	72
H(6A)	7480	7275	10779	96
H(6B)	6355	8586	10805	96
H(6C)	8281	8809	10575	96
H(7A)	3968	7625	9614	91
H(7B)	4605	6035	9633	91
H(9)	9865	6608	9835	71
H(10)	11345	5085	8967	73
H(11)	10230	4112	7597	67
H(12)	7637	4743	7212	58
H(14A)	2834	1557	7554	83
H(14B)	3834	1595	6690	83
H(14C)	1964	2033	6726	83
H(16A)	7250	5590	4956	146
H(16B)	7750	7278	5018	146
H(16C)	5914	6621	4689	146
H(18A)	-664	7882	7082	137
H(18B)	291	9441	7067	137
H(18C)	-289	8920	7953	137

¹ a) Hodgkins, T. G.; Powell, D. R. *Inorg. Chem.* **1996**, *35*, 2140-2148. b)

² Khaskin, E.; Zavalij, P.Y.; Vedernikov, A.N. *J. Am. Chem. Soc.* **2006**, *128*, 13054.

³ Alger, J. R.; Prestegard, J. H. *J. Magn. Reson.* **1977**, *27*, 137-141.

⁴ Derived from the Bloch-McConnell equations, H.M. McConnell, *J. Chem. Phys.* **1958**, *28*, 430.

⁵ Bain, A. D.; Cramer, J.A. *J. Magn. Reson.* **1996**, *118 A*, 21. CIFIT is available from Prof. Alex D. Bain, <http://www.chemistry.mcmaster.ca/bain/>.

⁶ Error tabulated according to Morse, P. M.; Spencer, M. D.; Wilson, S. R.; Girolami, G. S. *Organometallics* **1994**, *13*, 1646-1655.

⁷ Santhana Mariappan, S. V.; Rabenstein, D. L. *J. Magn. Reson.* **1992**, *100*, 183-188.

⁸ Sheldrick, G. M. *SHELXTL*, version 6.14; Bruker Analytical X-ray System, Inc.: Madison, WI, **1997**

⁹ Blessing, R.H. *Acta Crystallogr.* **1995**, *A51*, 33